JEM Journal of Experimental Medicine

ARTICLE

TRIM24 facilitates antiviral immunity through mediating K63-linked TRAF3 ubiquitination

Qingchen Zhu[1], Tao Yu[1], Shucheng Gan[1], Yan Wang[1], Yifei Pei[1], Qifan Zhao[1], Siyu Pei[1], Shumeng Hao[1], Jia Yuan[1], Jing Xu[1], Fajian Hou[2], Xuefeng Wu[3], Chao Peng[4], Ping Wu[4], Jun Qin[1], and Yichuan Xiao[1]

Ubiquitination is an essential mechanism in the control of antiviral immunity upon virus infection. Here, we identify a series of ubiquitination-modulating enzymes that are modulated by vesicular stomatitis virus (VSV). Notably, TRIM24 is down-regulated through direct transcriptional suppression induced by VSV-activated IRF3. Reducing or ablating TRIM24 compromises type I IFN (IFN-I) induction upon RNA virus infection and thus renders mice more sensitive to VSV infection. Mechanistically, VSV infection induces abundant TRIM24 translocation to mitochondria, where TRIM24 binds with TRAF3 and directly mediates K63-linked TRAF3 ubiquitination at K429/K436. This modification of TRAF3 enables its association with MAVS and TBK1, which consequently activates downstream antiviral signaling. Together, these findings establish TRIM24 as a critical positive regulator in controlling the activation of antiviral signaling and describe a previously unknown mechanism of TRIM24 function.

Introduction

Infection by RNA viruses, such as influenza and dengue viruses, remains a global threat to human health. Upon infection, viral RNA is recognized by host RNA sensors, such as retinoic acid inducible gene I (RIG-I), which initiates IFN-I signaling (Chiang et al., 2018; Goubau et al., 2013). After sensing viral RNA, RIG-I is recruited to interact with the downstream adaptor mitochondrial antiviral signaling protein (MAVS), which leads to the activation of TANK-binding kinase 1 (TBK1)/IFN regulatory factor 3/7 (IRF3/7), and finally the secretion of IFNα/β, members in a family of antiviral cytokines, to suppress virus propagation in vivo (Kawai et al., 2005; Meylan et al., 2005; Seth et al., 2005; Xu et al., 2005). In the battle between RNA viruses and their hosts, invading pathogens have evolved multiple strategies to counteract host antiviral immune signaling, such as inhibiting the recognition of viral RNA (Chan and Gack, 2016; Manokaran et al., 2015), preventing the binding between RIG-I and MAVS (He et al., 2016), or blocking the activation of TBK1 or IRF3 (Dalrymple et al., 2015; Zhu et al., 2019b), leading to promoted viral escape from host immune surveillance. However, the molecular events controlling the activation of host antiviral immune signaling remain poorly understood.

Ubiquitination is a type of posttranslational modification that has been found by numerous studies to play an important role in regulating host IFN-I signaling (Heaton et al., 2016; Khan et al., 2019; van Gent et al., 2018). Upon RNA virus infection, the signaling molecules in this pathway, such as RIG-I, MAVS, and TRAF3, undergo different types of ubiquitination by various E3 ubiquitin ligases and thus have different outcomes (Castanier et al., 2012; Gack et al., 2007; Mao et al., 2010; Tseng et al., 2010; Yan et al., 2014; Zhong et al., 2009). For example, K63-linked ubiquitination promotes the activation of downstream signaling and enhances the transcription of IFNα/β (Gack et al., 2007; Mao et al., 2010; Tseng et al., 2010; Yan et al., 2014), whereas K48-linked ubiquitination guides these molecules for proteasome degradation (Arimoto et al., 2007; Castanier et al., 2012; Zhong et al., 2009), generating a negative feedback loop to restrain IFN-I signaling. In addition, the ubiquitin that is added to these signaling molecules can be removed by deubiquitinases (DUBs) to counteract the effect of E3 ligase–induced ubiquitination (Cui et al., 2014; Friedman et al., 2008; Kayagaki et al., 2007; Pauli et al., 2014). Therefore, the dynamic regulation of the ubiquitination status of these signaling molecules by E3 ligases or DUBs fine-tunes the activation of IFN-I signaling.

Considering the critical fine-tuning role of ubiquitination in modulating IFN-I signaling, it is highly likely that the virus controls this cellular machinery by regulating the expression of

[1]Chinese Academy of Sciences Key Laboratory of Tissue Microenvironment and Tumor, Shanghai Institute of Nutrition and Health, Chinese Academy of Sciences, University of Chinese Academy of Sciences, Shanghai, China; [2]State Key Laboratory of Molecular Biology, Chinese Academy of Sciences Center for Excellence in Molecular Cell Science, Shanghai Institute of Biochemistry and Cell Biology, Chinese Academy of Sciences, University of Chinese Academy of Sciences, Shanghai, China; [3]Shanghai Institute of Immunology, Shanghai Jiao Tong University School of Medicine, Shanghai, China; [4]National Facility for Protein Science in Shanghai, Zhangjiang Lab, Shanghai, China.

Correspondence to Yichuan Xiao: ycxiao@sibs.ac.cn.

ubiquitination-related enzymes and thus modulates the host production of antiviral IFNα/β. In this study, we found that RNA virus–activated IRF3 suppresses the expression of tripartite motif 24 (TRIM24), an E3 ubiquitin ligase that mediates virus-induced K63-linked ubiquitination of TRAF3, leading to suppressed activation of downstream IFN-I signaling and thus antagonizing host antiviral immune responses.

Results

TRIM24 is down-regulated upon infection with vesicular stomatitis virus (VSV)

In an attempt to identify the potential ubiquitination-regulatory genes that are modulated by RNA viruses, we performed RNA-sequencing and quantitative PCR (QPCR) analysis and identified 49 up-regulated or down-regulated genes encoding E3 ligases or DUBs expressed at levels of significant difference ($\log2 \leq -1.5$ or $\log2 \geq 1.5$, $P < 0.005$) in murine primary macrophages infected with VSV (Fig. 1, A–C). Next, we knocked down the 49 differentially expressed E3 ligase or DUB genes in immortalized bone marrow–derived macrophages (iBMDMs) to examine VSV-induced *Ifnb1* gene expression. The results revealed that *TRIM24* and *Mib2* were the top two ubiquitination-regulatory genes to modulate VSV-induced *Ifnb1* expression (Fig. 1, D and E). Because a published study demonstrated a positive role for *Mib2* in regulating antiviral immunity (Ye et al., 2014), which validated our screening data, we focused our investigation on *TRIM24* in this study.

To confirm the role of TRIM24 in regulating VSV-induced *Ifnb1* expression, we knocked down *TRIM24* in iBMDMs by using two specific shRNAs and found that reducing TRIM24 expression indeed impaired *Ifnb1* induction upon VSV infection (Fig. 1, F and G). Accordingly, knocking down TRIM24 sharply promoted virus propagation, as reflected by enhanced GFP fluorescence, GFP protein expression, and virus titer after infection with GFP-conjugated VSV (Fig. 1, H–J). In contrast, TRIM24 overexpression dramatically curtailed virus propagation (Fig. 1, K–M). Together, these results identified TRIM24 as a VSV-modulated gene that exhibits a positive function in restraining virus propagation.

Loss of TRIM24 specifically impairs RNA virus–induced IFN-I production

Next, we generated *TRIM24* total knockout (hereafter termed *TRIM24*-KO) mice by crossing *TRIM24* floxed mice with mice expressing CMV-Cre recombinase, which is ubiquitously expressed in all cells and tissues (Fig. S1, A and B). Consistent with the knockdown data, *TRIM24* deficiency significantly suppressed the mRNA expression of *Ifna4*, *Ifnb1*, and IFN-stimulated genes (ISGs) in mouse primary macrophages infected with VSV or Sendai virus (SeV) and those transfected with polyI:C (Fig. 2 A and Fig. S1 C). In addition, VSV-induced IFNβ protein secretion was inhibited in *TRIM24*-deficient macrophages compared with WT cells (Fig. 2 B). Accordingly, loss of TRIM24 dramatically promoted virus propagation, as reflected by increased *VSV* mRNA expression and virus titer in VSV-infected *TRIM24*-deficient cells (Fig. 2, C and D). Interestingly, *TRIM24* deficiency did not affect the *Ifnb1* expression induced by LPS or herpes simplex virus 1 (HSV-1; Fig. 2 E), suggesting that TRIM24 specifically mediated RNA virus–induced, but was dispensable for TLR or DNA virus–induced, production of IFN-I.

We then examined the effect of TRIM24 in regulating RNA virus–induced activation of IFN-I signaling. In concert with the gene expression results, *TRIM24* deficiency markedly inhibited VSV- or transfected polyI:C-induced phosphorylation of TBK1 and IRF3 (Fig. 2, F and G). Accordingly, VSV-induced IRF3 dimerization and nuclear translocation were also dramatically suppressed in *TRIM24*-deficient primary mouse macrophages compared with WT cells (Fig. 2, H and I). More interestingly, knocking down *TRIM24* also inhibited VSV-induced *IFNB1* expression and promoted virus propagation in human peripheral blood mononuclear cell (PBMC)–derived macrophages (Fig. 2 J). However, *TRIM24* deficiency affected neither the VSV-induced activation of NF-κB or MAPKs nor the expression of STAT1 or proinflammatory genes (Fig. S1, D and E). These results collectively suggested that TRIM24 regulated RNA virus–induced activation of IFN-I signaling without affecting NF-κB or MAPK activation and thus specifically mediated IFN-I production.

TRIM24 deficiency impairs in vivo antiviral immunity

To study the in vivo function of TRIM24 in regulating antiviral immunity, WT and *TRIM24*-KO mice were infected with VSV. As expected, *TRIM24* deficiency significantly increased the VSV-induced mouse mortality rate and exaggerated immune cell infiltration and injury in the lungs (Fig. 3, A and B). In addition, the production of IFNα/β cytokines in the serum and their mRNA expression in the lungs and spleens were both significantly inhibited in the VSV-infected *TRIM24*-KO mice compared with WT controls (Fig. 3, C–E). Accordingly, loss of TRIM24 markedly promoted virus propagation in vivo after VSV infection, as reflected by increased VSV expression at both mRNA and protein levels in the lungs and spleens of VSV-infected *TRIM24*-deficient mice compared with WT control mice (Fig. 3, F and G). These data suggested that TRIM24 is critical for mediating in vivo antiviral immunity against VSV infection.

TRIM24 functions in mitochondria to mediate the antiviral response

Mitochondria are central hubs that dock antiviral-related signaling molecules to initiate the activation of downstream antiviral kinase cascades (Kawai et al., 2005; Meylan et al., 2005; Seth et al., 2005; Xu et al., 2005). To investigate whether TRIM24 also functions in mitochondria to regulate the antiviral immune response, immunofluorescence analysis was performed to examine the subcellular localization of TRIM24 upon virus infection. The results revealed that most of the TRIM24 protein (~80%) was localized in the nucleus of resting macrophages (Fig. 4, A and B). However, within 3 h of VSV infection, nuclear TRIM24 was translocated into the cytoplasm, leading to a dramatic change in subcellular localization such that ~40% of the TRIM24 protein was mobilized from the nucleus to the cytoplasm of the virus-infected cells (Fig. 4, A and B). In addition, the results from the immunoblot analysis confirmed that VSV infection gradually decreased nuclear TRIM24 protein levels but increased cytoplasmic TRIM24 protein levels (Fig. 4 C). More

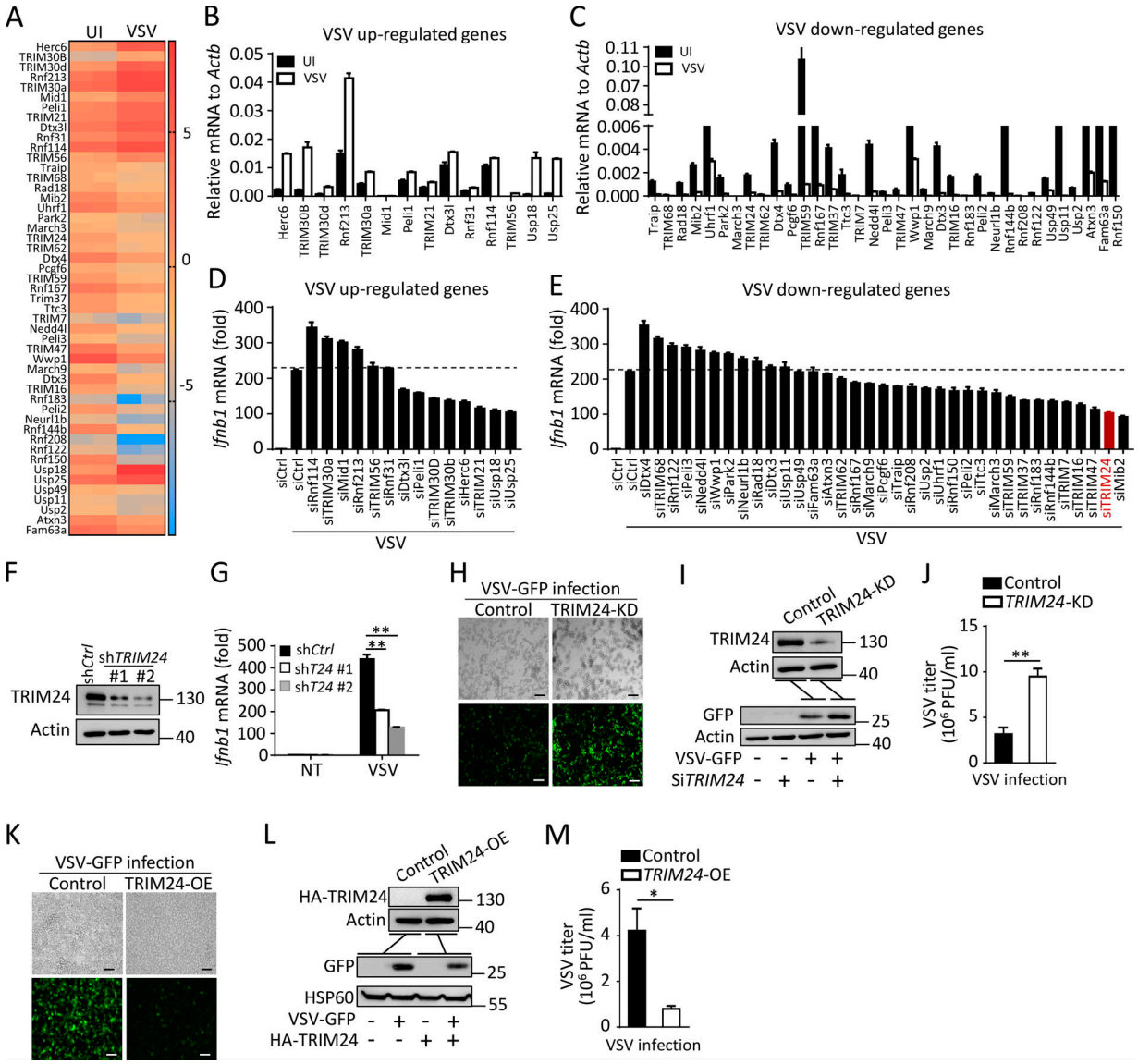

Figure 1. **Identification of TRIM24 as a VSV-modulated gene. (A)** RNA-sequencing analysis of the expression of genes in uninfected (UI) and VSV-infected BMDMs for 12 h. Heat map showing the normalized expression of the differentially expressed genes encoding E3 ligases and DUBs. **(B and C)** Real-time QPCR analysis confirming the expression levels of VSV up-regulated (B) or down-regulated (C) genes of E3 ligases and DUBs from A. The mRNA results are presented as the value relative to *Actb*. **(D and E)** Real-time QPCR analysis of *Ifnb1* expressions in uninfected and VSV-infected iBMDMs transfected with control siRNA (Ctrl) and siRNA targeting indicated VSV up-regulated (D) or down-regulated (E) genes. **(F and G)** Immunoblot analysis of TRIM24 protein expression (F) and QPCR analysis of VSV-induced *Ifnb1* mRNA expression in control (shCtrl) and *TRIM24* knockdown iBMDMs using two different shRNA targeting TRIM24 (sh*TRIM24* #1 and #2; G). NT, untreated. **(H–M)** Fluorescence microscopic, immunoblot analysis of virus infection efficiency, and virus titer assay in the culture supernatant of HEK293T cells transfected with control siRNA or siRNA targeting TRIM24 (TRIM24-KD) for 24 h, followed by infection with VSV-GFP for 24 h (H–J) or in HEK293T cells transfected with control or TRIM24-expressing vector (TRIM24-OE) for 24 h, followed by infection with VSV-GFP for 24 h (K–M). Scale bars, 100 µm. Data with error bars are represented as mean ± SEM. Each panel is a representative experiment of at least three independent biological replicates. *, P < 0.05; **, P < 0.01 as determined by unpaired Student's *t* test.

interestingly, with MitoTracker probes, we observed that VSV infection induced extensive localization of TRIM24 in mitochondria of peritoneal macrophages (Fig. 4, D–G), implying that TRIM24 was translocated to mitochondria upon virus infection to regulate antiviral immune signaling.

To determine the functional importance of TRIM24 translocation from the nucleus to the cytoplasm, we generated a mutant TRIM24 fusion protein with two nuclear localization signals (NLSs; Zhou et al., 2018) to ensure its maintenance in the nucleus, and then blocked its translocation to the cytoplasm. The immunofluorescence assay confirmed that TRIM24-NLS proteins were maintained in the nucleus with or without VSV infection, whereas the WT TRIM24 proteins were detected in both the nucleus and cytoplasm of 293T cells (Fig. 4 H). As expected, the TRIM24-NLS protein failed to promote RIG-I–induced IFNβ luciferase activity in HEK293T cells, in contrast to the promotion induced by WT TRIM24 (Fig. 4 I). Published studies have suggested that nuclear export protein chromosomal maintenance

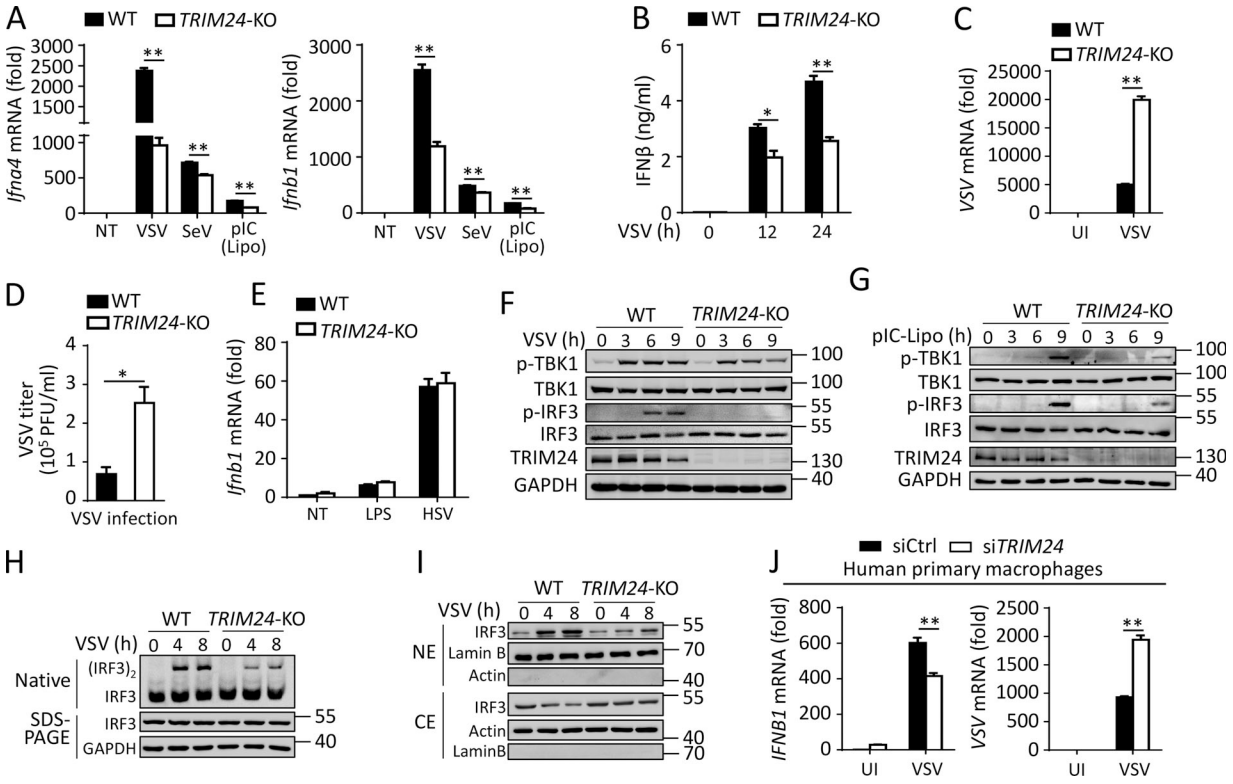

Figure 2. ***TRIM24* deficiency specifically inhibits RNA virus-induced antiviral signaling. (A)** QPCR analysis of *Ifna4* and *Ifnb1* in WT and *TRIM24*-KO peritoneal macrophages that were left untreated (NT) or infected with VSV or SeV or transfected with polyI:C (pIC) for 6 h. **(B)** ELISA of IFNβ protein levels in the supernatant of WT and *TRIM24*-KO peritoneal macrophages infected with VSV for the indicated times. **(C)** QPCR analysis of *VSV* mRNA in WT and *TRIM24*-KO peritoneal macrophages that were left uninfected (UI) or infected with VSV for 24 h. **(D)** Virus titer assay in the culture supernatant of WT and *TRIM24*-KO peritoneal macrophages infected with VSV for 24 h. **(E)** QPCR analysis of *Ifnb1* mRNA in WT and *TRIM24*-KO peritoneal macrophages that were left NT, stimulated with LPS, or infected with HSV-1 for 6 h. **(F and G)** Immunoblot analysis of phosphorylated and total TBK1 and IRF3 in whole-cell lysates of WT and *TRIM24*-KO peritoneal macrophages infected with VSV (F) or transfected with pIC (G) for the indicated time points. **(H)** Native gel analysis of IRF3 dimerization (above) and SDS-PAGE immunoblot of IRF3 and GAPDH (below) in whole-cell lysates of WT and *TRIM24*-KO peritoneal macrophages infected with VSV for indicated time points. **(I)** Immunoblot analysis of IRF3 in cytoplasmic (CE) and nuclear (NE) fractions of WT and *TRIM24*-KO peritoneal macrophages infected with VSV for indicated times. **(J)** QPCR analysis of *IFNB1* and *VSV* mRNA in human PBMC-derived primary macrophages transfected with control siRNA or siRNA targeting *TRIM24* for 24 h, followed by infection with VSV for 6 h. Data with error bars are represented as mean ± SEM. Each panel is a representative experiment of at least three independent biological replicates. *, P < 0.05; **, P < 0.01 as determined by unpaired Student's *t* test.

1 (CRM1) mediates the nucleocytoplasmic transportation of cargo proteins (Hutten and Kehlenbach, 2007). We found that TRIM24 was constitutively associated with CRM1 with or without VSV infection, and the TRIM24–CRM1 interaction was confirmed by using a transient transfection experiment in which TRIM24 overexpression was strongly associated with CRM1 (Fig. 4 J and Fig. S2 A). Moreover, the CRM1 selective inhibitor Kpt330 dramatically blocked TRIM24 transportation to the cytoplasm without affecting its overall cellular level, and thus, the differences in VSV-induced *Ifnb1* expression were abolished, as the mRNA levels in the WT and *TRIM24*-deficient mouse primary macrophages were reduced to a similar level (Fig. 4, K and L). Together, these data demonstrate that the translocation of TRIM24 from the nucleus to mitochondria is crucial for its antiviral activity.

TRIM24 mediates VSV-induced TRAF3 K63-linked ubiquitination

To figure out the direct molecular target of TRIM24 in IFN-I signaling, we performed a luciferase assay to examine IFNβ transcriptional activity after different key molecules in this signaling cascade were overexpressed with or without TRIM24 in HEK293T cells. The results revealed that TRIM24 significantly promoted RIG-I– and MAVS-induced IFNβ luciferase activity, whereas TRIM24 was dispensable for TBK1- or IRF3-induced IFNβ luciferase activity (Fig. 5 A), suggesting that TRIM24 targeted a molecule downstream of MAVS and upstream of TBK1. In concert with this result, knocking down *TRIM24* dramatically suppressed the *IFNB1* mRNA expression induced by overexpressed RIG-I and MAVS, whereas TRIM24 was found to be dispensable for the *IFNB1* mRNA expression induced by overexpressed TBK1 and IRF3 (Fig. 5 B). In addition, the results from the coimmunoprecipitation experiment confirmed that TRIM24 did not bind with overexpressed RIG-I, MAVS, TBK1, or IRF3 in HEK293T cells (Fig. 5 C). Moreover, TRIM24 did not associate with TRAF6 (Fig. 5 C), a MAVS downstream adaptor, to activate NF-κB or MAPK (Yoshida et al., 2008), which explained why TRIM24 was dispensable for VSV-induced proinflammatory gene expression. Interestingly, we found that TRIM24 coimmunoprecipitated with TRAF3, another MAVS downstream

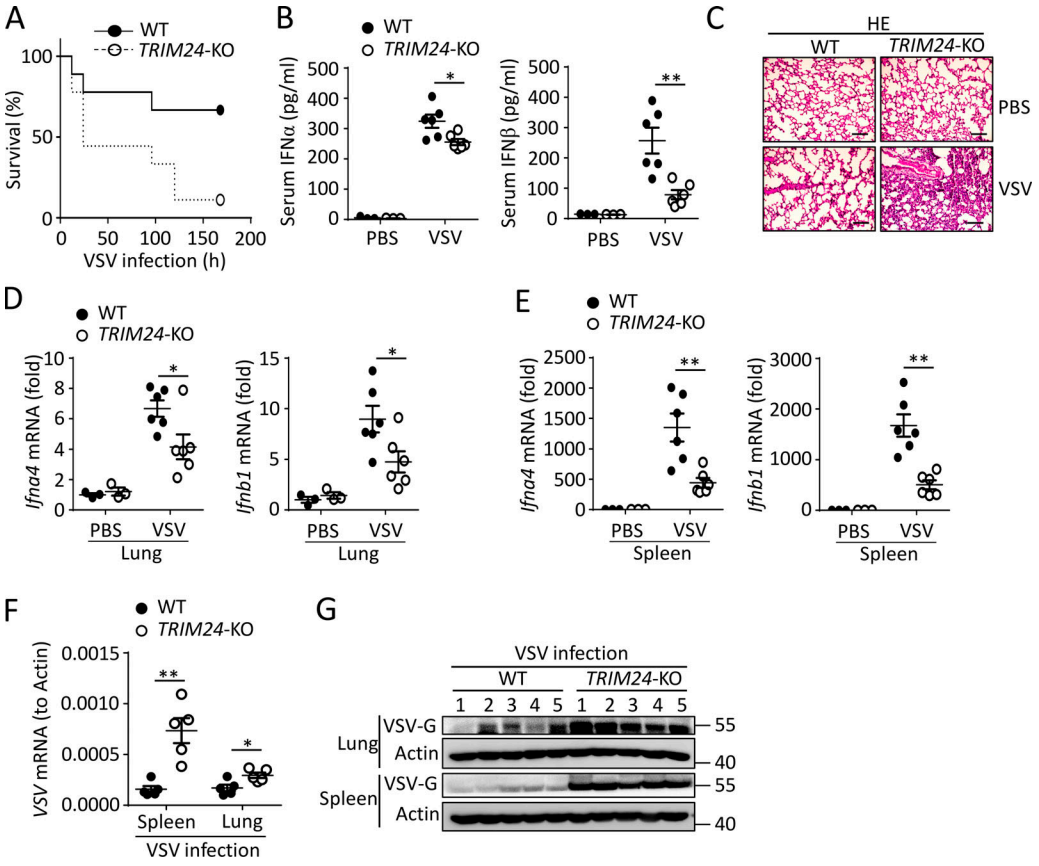

Figure 3. **Loss of TRIM24 impairs in vivo antiviral immunity. (A)** Survival of WT and *TRIM24*-KO mice (n = 9 mice/group) infected with VSV (1×10^8 PFU/mouse) via tail vein injection. **(B)** ELISA for IFNα and IFNβ in serum of WT and *TRIM24*-KO mice treated with PBS (n = 3 mice/group) or infected with VSV (n = 6 mice/group, 2.5×10^7 PFU/mouse) via tail vein injection for 12 h. **(C)** Representative H&E-stained images of lung sections from WT and *TRIM24*-KO mice infected with VSV (2.5×10^7 PFU/mouse) for 24 h. Scale bars, 100 µm. **(D and E)** QPCR analysis of *Ifna4* and *Ifnb1* mRNA in the lungs (D) and spleens (E) from the WT and *TRIM24*-KO mice (n = 6 mice/group) infected with VSV (2.5×10^7 PFU/mouse) via tail vein injection for 12 h. **(F and G)** QPCR analysis and immunoblot analysis of *VSV* expression in the lungs and spleens from the WT and *TRIM24*-KO mice infected with VSV (2.5×10^7PFU/mouse) for 24 h. Data with error bars are represented as mean ± SEM. Each panel is a representative experiment of at least three independent biological replicates. *, $P < 0.05$; **, $P < 0.01$ as determined by unpaired Student's t test.

adaptor, to transduce antiviral signaling that mediates IFN-I transcription in HEK293T cells, in which these two proteins were overexpressed (Fig. 5 D). The TRIM24–TRAF3 association was confirmed in mouse primary macrophages, in which the two molecules were found to bind to each other in resting cells and VSV-infected cells (Fig. 5 E).

Next, plasmids encoding full-length or truncated TRIM24 were generated to investigate the functional domain that contributes to TRIM24-mediated antiviral immunity (Fig. 5 F). The results revealed that deleting the C-terminal of TRIM24, which lacks the pleckstrin homology domain and bromodomain, did not affect its ability to promote MAVS-induced IFNβ luciferase activity, whereas an N-terminal–truncated TRIM24 construct that lacked the ring domain failed to boost MAVS-mediated *IFNB1* transcription (Fig. 5 G). In addition, reconstitution of the N-terminal–deleted TRIM24 failed to restore VSV-induced *Ifnb1* expression in *TRIM24*-KO macrophages to the same level as that induced by full-length TRIM24 (Fig. 5 H). These results suggest that ring domain–related E3 ligase activity is critical for TRIM24-mediated antiviral activity.

Considering the interaction between TRIM24 and TRAF3, we speculated that TRIM24 functions as an E3 ligase of TRAF3 to mediate antiviral immunity. Indeed, overexpression of TRIM24 specifically promoted the K63-linked ubiquitination, but not other types (K6-, K11-, K27-, K29-, K33-, or K48-linked), of TRAF3 (Fig. 6 A and Fig. S2, B and C). In addition, overexpression of full-length TRIM24, but not a ring domain–deleted mutant (TRIM24ΔN), markedly enhanced TRAF3 ubiquitination (Fig. 6 B). Moreover, overexpression of TRIM24 also promoted K63-linked ubiquitination of the C68A/H70A mutant TRAF3 (Fig. 6 C), indicating that TRIM24-mediated TRAF3 ubiquitination is independent of its autoubiquitination activity. Consistently, *TRIM24* deficiency dramatically suppressed VSV-induced endogenous K63-linked TRAF3 ubiquitination in mouse primary macrophages, as determined through separate pull-down assays of TRAF3 and ubiquitin (Fig. 6, D and E). Furthermore, an in vitro ubiquitination assay confirmed that the TRIM24 protein could directly and specifically add to the polyubiquitin chains in the in vitro cell-free translated TRAF3 protein but not to those in the TRAF2 protein (Fig. 6, F and G; and Fig. S2 D), suggesting that

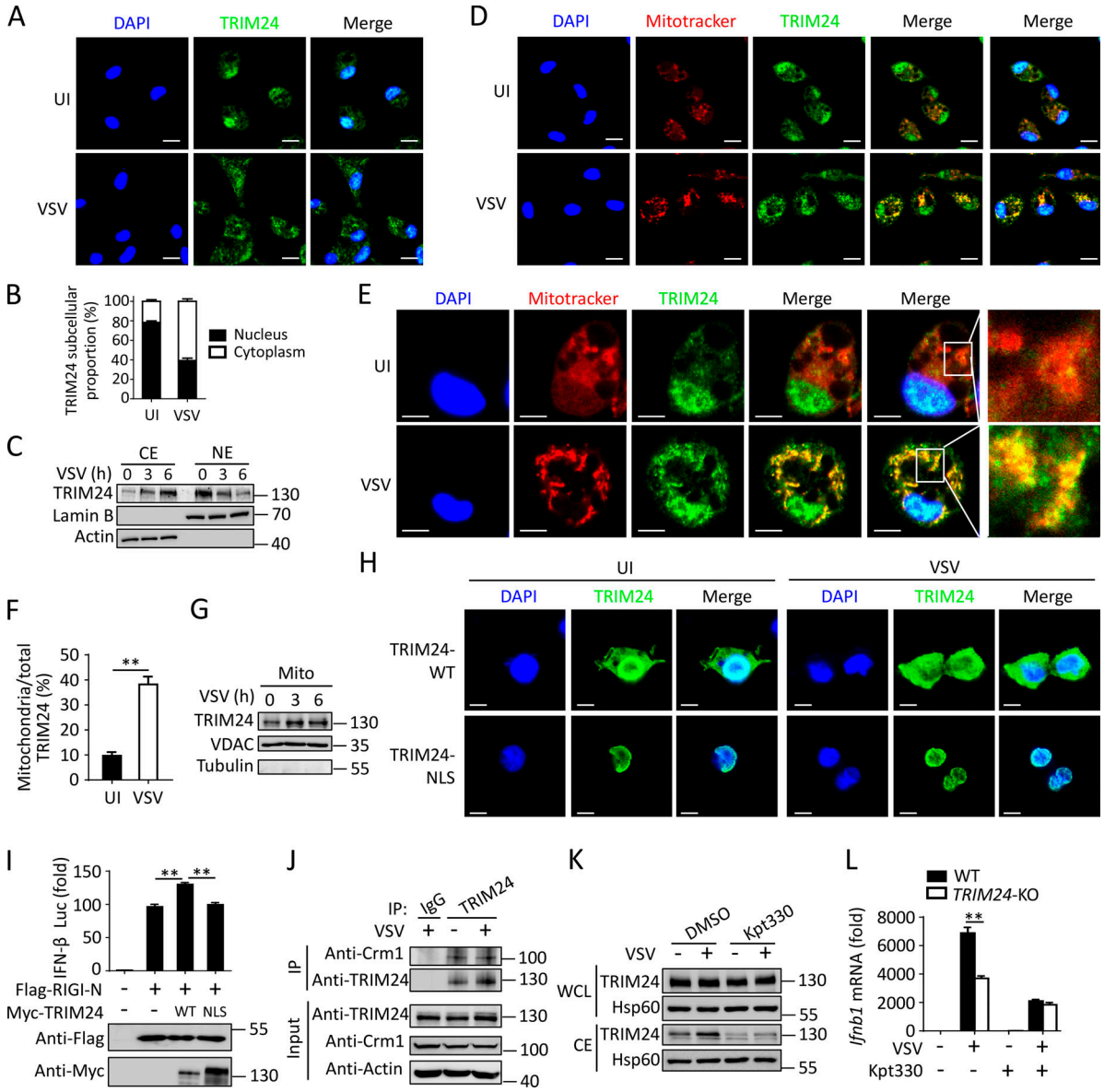

Figure 4. **TRIM24 is translocated from nucleus to mitochondria to mediate antiviral immunity. (A and B)** Confocal microscopic images and quantification of relative TRIM24 subcellular proportion of peritoneal macrophages left uninfected (UI) or infected with VSV for 3 h and probed with the DNA-binding dye DAPI and anti-TRIM24. Scale bars, 10 µm. **(C)** Immunoblot analysis of TRIM24 in cytoplasmic (CE) and nuclear (NE) fractions of peritoneal macrophages infected with VSV for the indicated time points. **(D and E)** Confocal microscopic and immunoblot analysis of TRIM24 localization in peritoneal macrophages that were left uninfected or infected with VSV for 3 h and probed with DAPI, anti-TRIM24, and MitoTracker Deep Red FM. Scale bars, 10 µm (D); 2 µm (E). **(F)** Percentages of TRIM24 localization in mitochondria relative to total TRIM24 in cells were quantified based on the images obtained in E. **(G)** Immunoblot analysis of TRIM24 and VDAC (loading control) in mitochondria of peritoneal macrophages infected without or with VSV for the indicated time points. **(H)** Confocal microscopic images of HEK293T cells transfected with Myc-TRIM24-WT or Myc-TRIM24-NLS expression vectors and then left uninfected or infected with VSV and probed with anti-Myc. Scale bars, 5 µm. **(I)** IFNβ luciferase activity in HEK293T cells transfected with luciferase reporter and indicated expression vectors including Myc-TRIM24, Myc-TRIM24-NLS, or RIG-I N-terminal 2CARD (RIGI-N; upper), and immunoblot of the protein levels of transfected vectors (lower). **(J)** Immunoblot analysis of TRIM24–CRM1 interaction in peritoneal macrophages left uninfected or infected with VSV, assessed by immunoprecipitation (IP) with anti-IgG or anti-TRIM24, immunoblotting (IB) with anti-TRIM24 or anti-CRM1, and immunoblot analysis with input proteins in lysates and loading controls without immunoprecipitation. **(K)** Immunoblot analysis of TRIM24 in the whole-cell lysis (WCL) and cytoplasmic (CE) fractions of peritoneal macrophages left uninfected (–) or infected (+) with VSV after treatment with DMSO or CRM1 selective inhibitor Kpt330 for 4 h. **(L)** QPCR analysis of *Ifnb1* mRNA in WT and *TRIM24*-KO peritoneal macrophages left uninfected or infected with VSV after treatment with DMSO or Kpt330 for 4 h. Data with error bars are represented as mean ± SEM. Each panel is a representative experiment of at least three independent biological replicates. *, P < 0.05; **, P < 0.01 as determined by unpaired Student's *t* test.

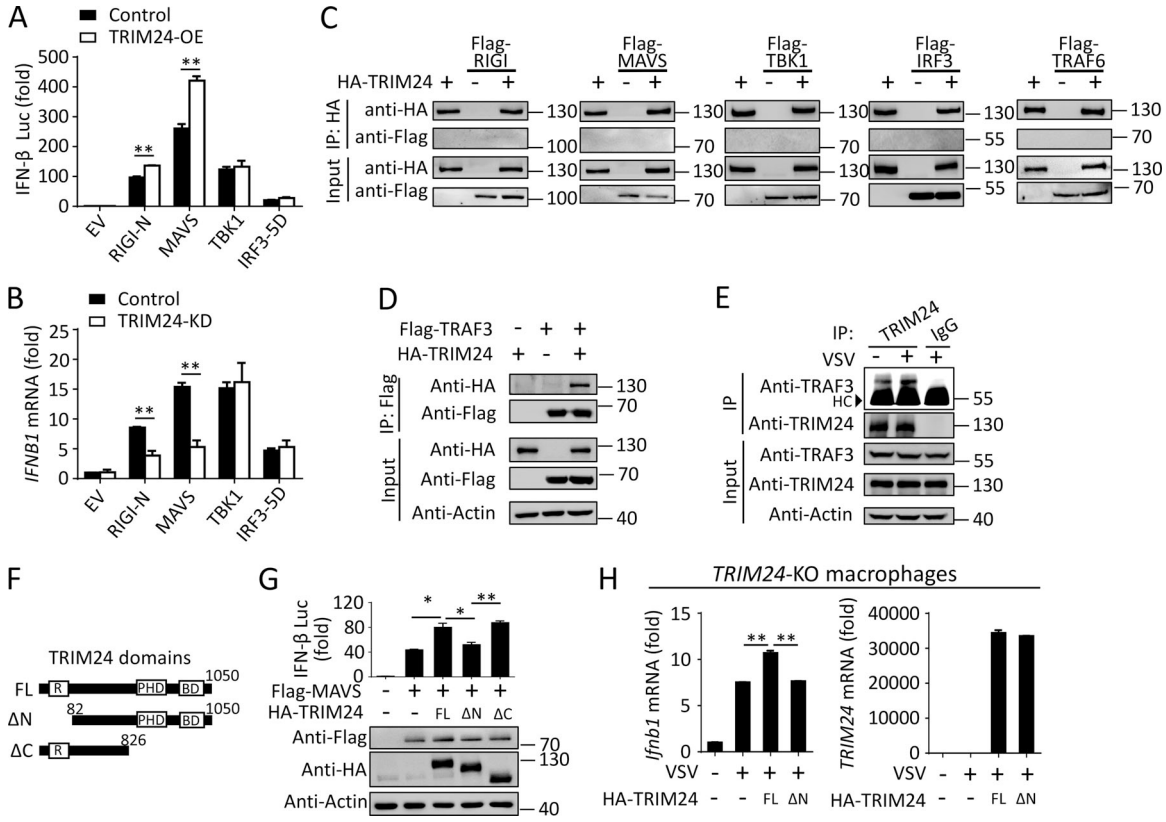

Figure 5. **TRIM24 RING domain contributes to its antiviral function. (A)** IFNβ luciferase activity in control and HA-TRIM24 overexpressed (OE) HEK293T cells transfected with luciferase reporter and indicated expression plasmids for RIGI-N, MAVS, TBK1, or IRF3-5D. **(B)** QPCR analysis of *IFNB1* mRNA expression in HEK293T cells transfected for 24 h with control or TRIM24-specific siRNA (KD), together with expression plasmids for RIGI-N, MAVS, TBK1 or IRF3-5D. **(C)** Immunoblot analysis to screen TRIM24-associated proteins in HEK293T cells transfected with the indicated expression vectors, assessed by immunoprecipitation (IP) with anti-HA and immunoblotting (IB) with anti-HA and anti-Flag, and by immunoblot analysis with input proteins in lysates without immunoprecipitation. **(D and E)** Immunoblot analysis of TRIM24–TRAF3 interaction in HEK293T cells transfected with the indicated expression vectors (D), and in peritoneal macrophages left uninfected or infected with VSV (E), assessed by IP with anti-Flag, anti-IgG, or anti-TRIM24 and by IB with anti-HA and anti-Flag, or with anti-TRIM24 and anti-TRAF3, and by immunoblot analysis with input proteins in lysates and loading controls without immunoprecipitation. **(F and G)** IFNβ luciferase activity in HEK293T cells transfected with luciferase reporter, Flag-MAVS, and the expressing vectors encoding full-length (FL), N-terminal (ΔN), or C-terminal (ΔC) truncated HA-TRIM24. The structure schema of FL TRIM24 and its truncations is shown in F, and the luciferase activities and immunoblot of the protein levels of transfected vectors was shown in G. **(H)** QPCR analysis of *Ifnb1* and *TRIM24* mRNA expression in TRIM24-KO macrophages reconstituted with empty vector (–), FL-TRIM24, and TRIM24ΔN and then left uninfected (–) or infected with VSV (+) for 6 h. Data with error bars are represented as mean ± SEM. Each panel is a representative experiment of at least three independent biological replicates. *, P < 0.05; **, P < 0.01 as determined by unpaired Student's *t* test.

TRIM24 is a direct E3 ligase that mediates the K63-linked ubiquitination of TRAF3.

Because K63-linked ubiquitination is known to serve as a docking site for signaling molecules (Wang et al., 2012), it is reasonable to speculate that K63-linked ubiquitination of TRAF3 enhances its binding with antiviral-related signaling molecules. Indeed, we found that overexpression of TRIM24 promoted the binding of TRAF3 with MAVS or TBK1 in a dose-dependent manner in HEK293T cells that transiently expressed these proteins (Fig. S2, E and F). Additionally, loss of TRIM24 dramatically suppressed the VSV-induced endogenous association of TRAF3 with MAVS or TBK1 (Fig. 6 H), which explains why TRIM24 docks at mitochondria to mediate the activation of antiviral signaling upon VSV infection. Therefore, these results collectively suggest that TRIM24-mediated K63-linked ubiquitination of TRAF3 facilitates the downstream signal transduction of the IFN-I pathway.

TRAF3 K429/436 ubiquitination is critical for TRIM24-mediated antiviral immunity

We next performed mass spectrometry analysis of Flag-tagged TRAF3 in the presence of TRIM24 overexpression and identified K369, K429, and K436 as potential ubiquitination sites targeted by TRIM24 (Fig. 7 A and Fig. S3). We subsequently generated a series of corresponding TRAF3 point mutations and found that TRIM24 failed to promote the ubiquitination of the K429R or K436R single- or double-point mutated TRAF3 (Fig. S4, A and B), indicating that K429 and K436 are the actual ubiquitination sites targeted by TRIM24. Accordingly, the K429R and K436R TRIM24 mutants were less efficient than WT TRAF3 in promoting RIG-I–induced IFNβ luciferase activity, and the K429/436R double-point mutation impaired the ability of TRAF3 to boost RIG-I activity to a greater extent than did the single-point mutation (Fig. S4 C). In addition, the reconstitution of the K429/436R TRAF3 mutant in *TRAF3*-deficient mouse embryonic fibroblasts

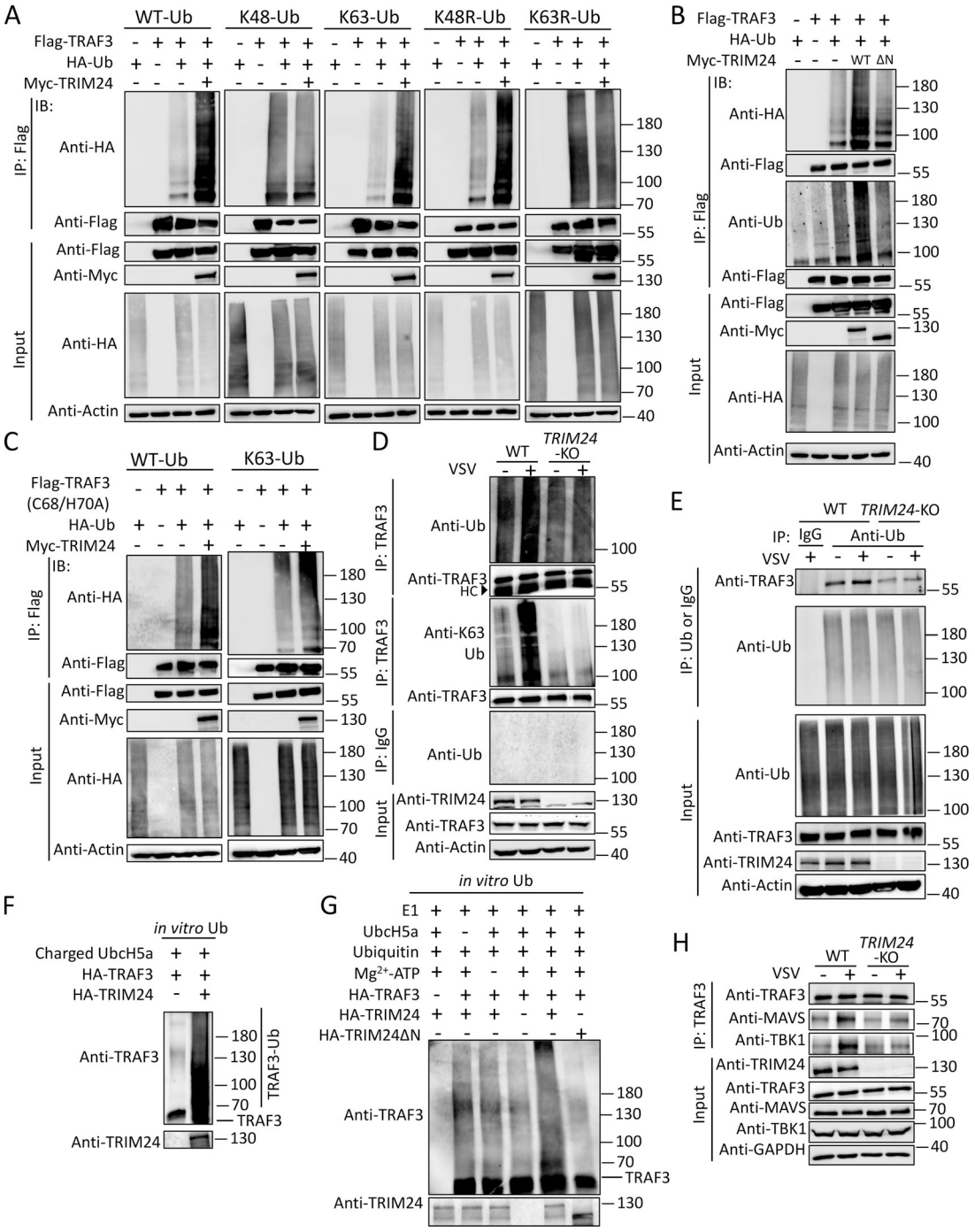

Figure 6. **TRIM24 mediates K63-linked ubiquitination of TRAF3. (A–C)** Ubiquitination of TRAF3 in HEK293T cells transfected with the indicated expression vectors, assessed by immunoblot analysis (IB) with anti-HA or anti-ubiquitin (Ub) after immunoprecipitation (IP) with anti-Flag or by immunoblot analysis with input proteins in lysates without immunoprecipitation. **(D)** Endogenous ubiquitination of TRAF3 in WT and *TRIM24*-KO peritoneal macrophages that were left uninfected (–) or infected (+) with VSV for 6 h, assessed by immunoblot analysis with anti-Ub or anti-K63 Ub or anti-TRAF3 after immunoprecipitation with anti-TRAF3 or control IgG, and by immunoblot analysis with input proteins and loading control. **(E)** Immunoblot analysis of endogenous TRAF3 ubiquitination in WT and *TRIM24*-KO peritoneal macrophages that were left uninfected (–) or infected (+) with VSV for 6 h, assessed by immunoblot analysis with anti-TRAF3 or anti-Ub after immunoprecipitation with anti-Ub or control IgG, and by immunoblot analysis with input proteins and loading control. **(F and G)** In vitro ubiquitination assay of TRAF3 ubiquitination after a mixture reaction of ubiquitin-charged E2 (UbcH5a) or uncharged E2 (UbcH5a) with E1, ubiquitin, Mg^{2+}-ATP, in vitro translated HA-TRAF3, and with or without HA-TRIM24 or HA-TRIM24ΔN proteins, assessed by immunoblot analysis with anti-TRAF3 and anti-TRIM24. **(H)** Immunoblot analysis of TRAF3-associated proteins in WT and *TRIM24*-KO peritoneal macrophages that were left uninfected (–) or infected (+) with VSV for 6 h, assessed by IP with anti-TRAF3, by IB with anti-TRAF3, anti-MAVS, and anti-TBK1, and by immunoblot analysis with input proteins in lysates and loading controls without immunoprecipitation. Data with error bars are represented as mean ± SEM. Each panel is a representative experiment of at least three independent biological replicates. *, P < 0.05; **, P < 0.01 as determined by unpaired Student's *t* test.

(MEFs) failed to recover VSV-induced *Ifna4* and *Ifnb1* mRNA expression to the level that WT TRAF3 did (Fig. S4, D and E).

To confirm the importance of endogenous TRAF3 K429/436 ubiquitination, we generated K429/436R double knock-in HEK293T cells with both copies of the mutant *TRAF3* gene by using the CRISPR/Cas9 system and verified the mutations by sequencing the genomic DNA (Fig. 7 B). K429/436R knock-in did not affect the endogenous protein expression levels of TRAF3, MAVS, or IRF3 (Fig. S4 F). However, this knock-in mutation dramatically suppressed RIG-I overexpression–induced IFNβ luciferase activity, whereas it was dispensable for TIR domain-containing adapter-inducing IFNβ (TRIF)– and stimulator of IFN genes (STING)–induced IFNβ luciferase activity (Fig. 7 C), confirming that TRIM24-induced TRAF3 K429/436 ubiquitination specifically regulated VSV-induced IFN-I expression. In addition, TRIM24 overexpression failed to promote RIG-I–induced IFNβ luciferase activity in the K429/436R knock-in HEK293T cells to the level it was expressed in the WT cells (Fig. 7 D). We next examined the ubiquitination status of TRAF3 and found that the TRAF3 K429/436R knock-in nearly abolished the endogenous ubiquitination induced by VSV infection (Fig. 7 E). Accordingly, the VSV-induced interaction of TRAF3 with MAVS, TBK1, and IRF3 phosphorylation, dimerization, and nuclear translocation were greatly inhibited in the TRAF3 K429/436R knock-in cells (Fig. 7, F–H). As a consequence, VSV-induced IFNβ luciferase activity and *IFNB1* mRNA expression were dramatically suppressed, and virus propagation was significantly enhanced in the TRAF3 K429/436R knock-in cells (Fig. 7, I–K). These results collectively established a critical role for TRIM24-induced TRAF3 K429/436 ubiquitination in mediating antiviral immunity against RNA viruses.

RNA virus–activated IRF3 suppresses *TRIM24* transcription

Because our data established a key role of TRIM24 in fighting against RNA viruses, we next sought to investigate how TRIM24 is modulated upon virus infection. We found that VSV infection gradually decreased both the mRNA and protein levels of TRIM24 in a time-dependent manner in mouse primary macrophages, suggesting that VSV suppressed *TRIM24* expression at the transcriptional level (Fig. 8, A and B). VSV infection also inhibited *TRIM24* mRNA expression in human PBMC-derived primary macrophages (Fig. 8 C). In addition, *TRIM24* mRNA expression was significantly suppressed in different types of human cells upon infection with various RNA viruses, such as respiratory syncytial virus (RSV) and H1N1 influenza virus (Fig. 8, D and E), implying that the suppression of *TRIM24* expression was not specific to VSV infection.

RNA virus infection induces the activation and nuclear translocation of IRF3, NF-κB, and activator protein 1 (AP-1) to modulate gene transcription (Chiang et al., 2018; Goubau et al., 2013; Kawai et al., 2005; Meylan et al., 2005; Seth et al., 2005; Xu et al., 2005), which prompted us to examine whether these transcription factors directly contribute to TRIM24 suppression. The results revealed that inhibition of NF-κB– or AP-1–related kinases (ERK, JNK, or p38) through corresponding selective inhibitors did not restore *TRIM24* expression upon VSV infection (Fig. 8 F). Interestingly, we found that infection by the HSV-1 DNA virus also suppressed *TRIM24* mRNA expression in a time-dependent manner in mouse primary macrophages (Fig. 8 G), which prompted us to speculate that IRF3, a transcription factor that is activated by both DNA and RNA viruses, may mediate TRIM24 transcriptional suppression. Indeed, we found that VSV infection failed to inhibit *TRIM24* expression and completely abolished *IFNB1* induction in *IRF3*-deficient HEK293T cells, and reconstitution of IRF3 restored both VSV-induced *TRIM24* suppression and *IFNB1* expression (Fig. 8, H and I), suggesting that virus-activated IRF3 contributed to the suppression of TRIM24 in the host cells.

To confirm the direct transcriptional inhibitory function of IRF3 on *TRIM24* expression, we generated luciferase reporter plasmids by introducing different mouse *TRIM24* promoter fragments into a pGL4-basic plasmid (Fig. 8 J) and found that the promoter region between −3,813 and −2,256 contributed to the basal expression of *TRIM24* (Fig. 8 K). In addition, we also determined that the promoter region between −3,813 and −2,804 effectively responded to VSV infection to suppress *TRIM24* transcription (Fig. 8 L), and *IRF3* deficiency abolished VSV-induced transcriptional suppression of this promoter region (Fig. 8 M). As expected, a conserved IRF3-binding motif was found in the promoter region between −3,813 and −2,804 (Fig. 8 N), and the chromatin immunoprecipitation (ChIP)–QPCR experiment results also confirmed that VSV infection induced abundant IRF3 binding to the *TRIM24* promoter region and to the *IFNB1* gene promoter (Fig. 8 O). Moreover, IRF3 failed to suppress *TRIM24* transcription and could not efficiently bind to the DNA sequence when four bases of the IRF3-binding motif were mutated (Fig. 8, P and Q). Together, these data demonstrated that the RNA virus suppressed *TRIM24* transcription directly by activated IRF3.

Discussion

Although RNA virus infection induces swift activation of host innate immunity to produce IFN-I, long-term infection impairs the expression of host antiviral cytokines, leading to uncontrolled virus propagation (Chan and Gack, 2016; Dalrymple et al., 2015; He et al., 2016; Manokaran et al., 2015; Zhu et al., 2019b). TRIM family proteins play crucial roles in modulating innate antiviral immunity and are thus essential for fighting against viral infection (van Gent et al., 2018). Interestingly, a screening study of all TRIM family proteins demonstrated that TRIM24 positively regulates RIG-I–induced IFNβ luciferase activity by using an overexpression system (Versteeg et al., 2013), the findings of which were confirmed by our current study at the genetic level: *TRIM24* deficiency indeed impaired RNA virus–induced IFN-I induction and in vivo antiviral immunity. Our findings suggested that TRIM24 functions as a positive regulator to mediate the activation of IRF3 for antiviral immunity, and that it can also be transcriptionally suppressed by activated IRF3 directly, which forms a classic negative feedback loop to restrain the overactivation of antiviral IFN signaling. We speculated that IRF3-induced down-regulation of *TRIM24* is mediated through its recruitment of transcriptional coinhibitors to the promoter region of the *TRIM24* gene, a supposition that needs further investigation in future studies.

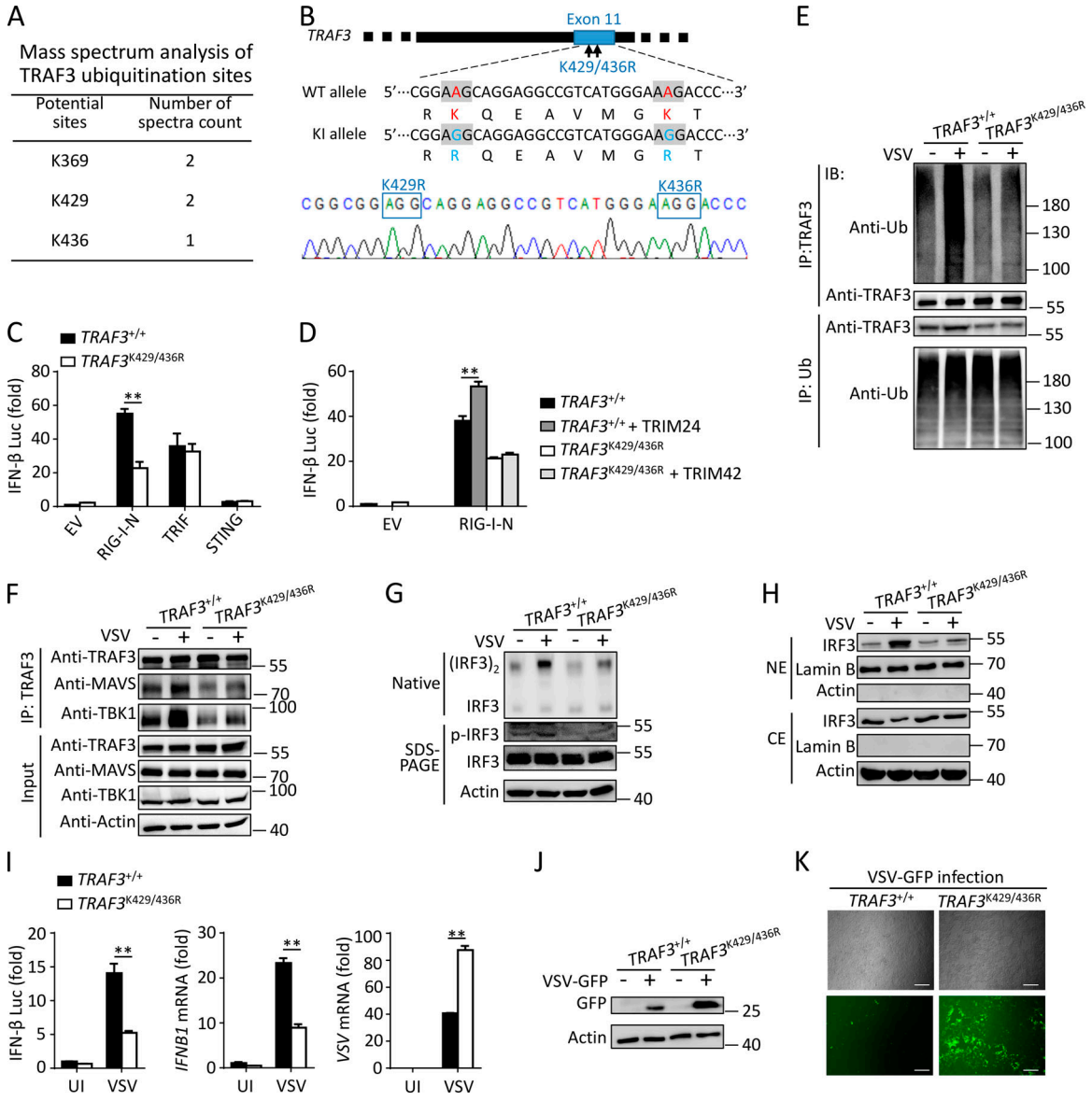

Figure 7. **TRAF3 K429/K436 ubiquitination is critical for TRIM24-mediated antiviral immunity. (A)** Mass spectrum analysis showing the potential ubiquitination sites of TRAF3 after immunoprecipitation of TRAF3 in HEK293T cells transfected with Flag-TRAF3, Myc-TRIM24, and HA-ubiquitin. **(B)** Knock-in strategy (upper panel) and sequencing verification of the codon replacement (lower panel) for TRAF3-K429R/K436R by using CRISPR/Cas9 technique. **(C and D)** IFNβ luciferase activity in WT (*TRAF3*$^{+/+}$) and TRAF3-K429R/K436R knock-in (*TRAF3*$^{K429/436R}$) HEK293T cells transfected with luciferase reporter and indicated expression vectors. **(E)** Endogenous ubiquitination of TRAF3 in *TRAF3*$^{+/+}$ and *TRAF3*$^{K429/436R}$ HEK293T cells that were left uninfected (–) or infected (+) with VSV, assessed by immunoblot (IB) analysis with anti-ubiquitin or anti-TRAF3 after immunoprecipitation (IP) with anti-TRAF3 or anti-ubiquitin. **(F)** Immunoblot analysis of TRAF3-associated proteins in *TRAF3*$^{+/+}$ and *TRAF3*$^{K429/436R}$ HEK293T cells that were left uninfected (–) or infected (+) with VSV, assessed by immunoprecipitation with anti-TRAF3, by immunoblot with anti-TRAF3, anti-MAVS, and anti-TBK1, and by immunoblot analysis with input proteins in lysates and loading controls without immunoprecipitation. **(G and H)** Native gel analysis of IRF3 dimerization (above) and SDS-PAGE immunoblot of phosphorylated (p) and total IRF3 and GAPDH (below) in whole-cell lysates (G), and immunoblot analysis of IRF3 in cytoplasmic (CE) and nuclear (NE) fractions (H) of *TRAF3*$^{+/+}$ and *TRAF3*$^{K429/436R}$ HEK293T cells left uninfected (–) or infected (+) with VSV. **(I)** IFNβ luciferase activity and QPCR analysis of *IFNB1* and *VSV* mRNA in *TRAF3*$^{+/+}$ and *TRAF3*$^{K429/436R}$ HEK293T cells that were left uninfected (UI) or infected with VSV for 24 h. **(J and K)** Immunoblot of GFP (J) and fluorescence microscopy of GFP fluorescence (K) in *TRAF3*$^{+/+}$ and *TRAF3*$^{K429/436R}$ HEK293T infected with VSV-GFP for 24 h. Scale bars, 100 µm. Data with error bars are represented as mean ± SEM. Each panel is a representative experiment of at least three independent biological replicates. *, P < 0.05; **, P < 0.01 as determined by unpaired Student's *t* test.

A previous study revealed that TRIM24 negatively regulates STAT1 expression and then further inhibits ISG expression in liver tissues through direct transcriptional suppression in the nucleus (Tisserand et al., 2011). However, our study demonstrated that TRIM24 in macrophages does not affect STAT1 expression but functions in the mitochondria to promote IFN-I and ISG expression. This functional difference may be due to the cell-specific mechanism of TRIM24 to regulate ISG expression. In addition to these findings on TRIM24, our RNA-sequencing experiment also enabled us to identify a number of differentially

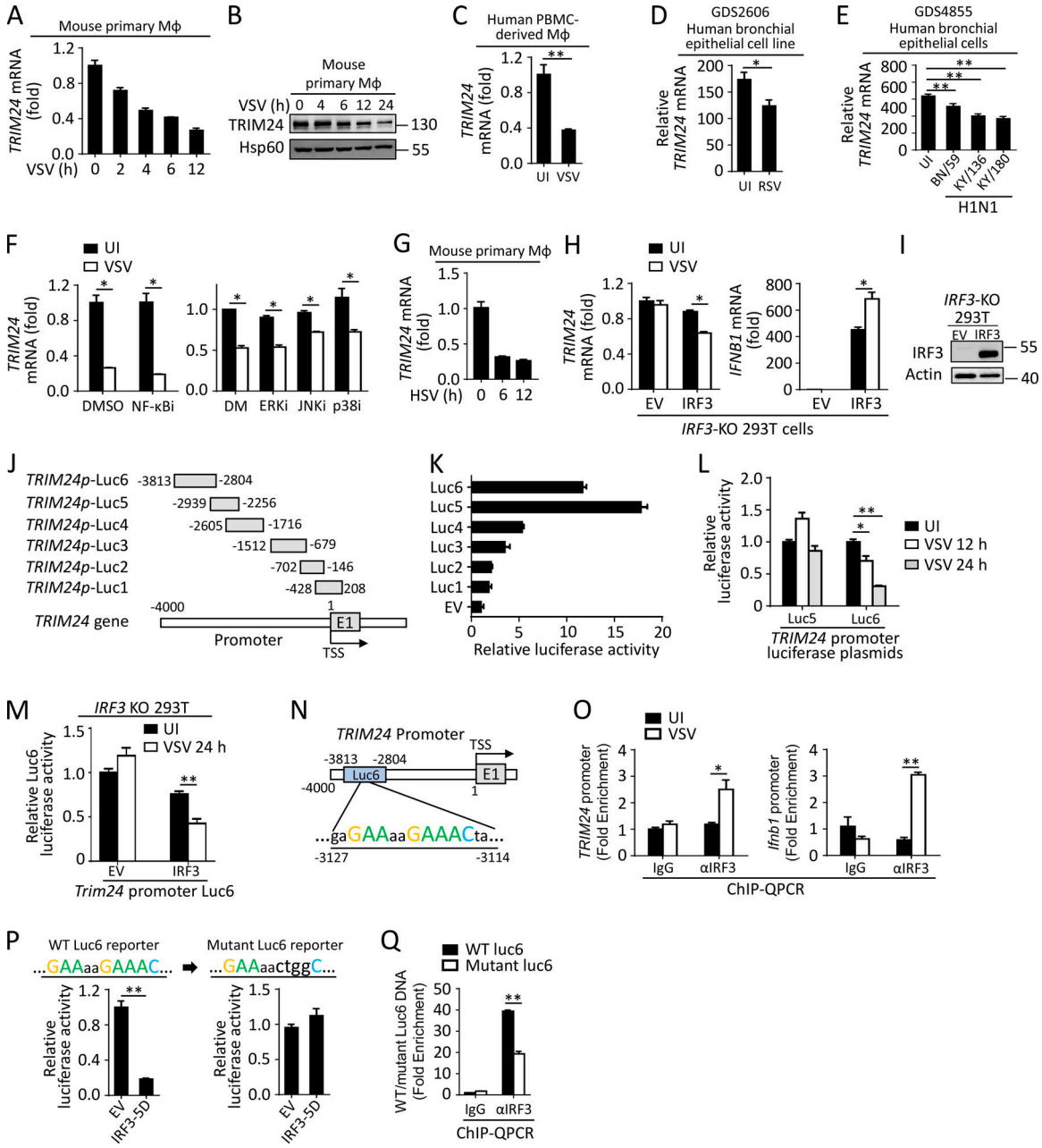

Figure 8. **VSV-activated IRF3 directly suppresses *TRIM24* transcription. (A–C)** QPCR analysis of *TRIM24* mRNA (A) and immunoblot of TRIM24 protein (B) in mouse primary macrophages (Mφ), or qPCR analysis of *TRIM24* mRNA in human PBMC-derived Mφ (C) left uninfected (UI) or infected with VSV for the indicated times. **(D and E)** Relative *TRIM24* expression in human bronchial epithelial cells left uninfected or infected with RSV (D) or H1N1 (E); data were obtained from the National Center for Biotechnology Information Gene Expression Omnibus database (GDS2606, GDS4855, GDS4387). **(F)** QPCR analysis of *TRIM24* mRNA in mouse primary peritoneal macrophages left uninfected or infected with VSV after treatment with DMSO (DM) or different selective inhibitors against NF-κB (pyrrolidinedithiocarbamate ammonium), ERK (PD98059), JNK (SP600125), or p38 (SB203580). **(G)** QPCR analysis of *TRIM24* mRNA in mouse primary Mφ infected with HSV-1 for the indicated times. **(H)** QPCR analysis of *TRIM24* and *IFNB1* mRNA in *IRF3*-KO HEK293T cells reconstituted with empty vector (EV) or Flag-IRF3, followed by UI or infection with VSV for 24 h. **(I)** Immunoblot of IRF3 in *IRF3*-KO HEK293T cells that reconstituted with EV or Flag-IRF3. **(J and K)** Structure schema of the constructed luciferase reporter by using different truncated promoter sequences of *TRIM24* genes (J), which were then used to test the transcriptional activity of *TRIM24* (K). **(L and M)** Luciferase activity of *TRIM24* transcriptional activity in HEK293T cells that were transfected with *TRIM24p*-Luc5 (−2,939/−2,256)– or *TRIM24p*-Luc6 (−3,813/−2,804)–driven luciferase reporter, then left uninfected or infected with VSV for the indicated times (L), or in *IRF3*-KO HEK293T cells reconstituted with EV or Flag-IRF3, transfected with *TRIM24p*-Luc6 (−3,813/−2,804)–driven luciferase reporter, then left uninfected or infected with VSV for the indicated times (M). **(N)** Schematic representation showing a conserved IRF3-binding motif located in the promoter region of *TRIM24* genes between −3,127 and −3,114. **(O)** ChIP-QPCR analysis of the binding activity of IRF3 in the promoter region of *TRIM24* and *Ifnb1* gene in mouse peritoneal macrophages left uninfected or infected with VSV for 6 h. **(P and Q)** Luciferase assay of *TRIM24* transcriptional activity (P) or ChIP-QPCR analysis of IRF3 binding activity (Q) in HEK293T cells that were transfected with WT *TRIM24p*-Luc6- (left) or mutant *TRIM24p*-Luc6–driven luciferase reporter (right), together with the EV or expression vector encoding IRF3-5D. Data with error bars are represented as mean ± SEM. Each panel is a representative experiment of at least three independent biological replicates. *, P < 0.05; **, P < 0.01 as determined by unpaired Student's *t* test.

expressed ubiquitination-regulatory genes that were modulated upon virus infection. The overall effect of these virus-modulated ubiquitination-regulator genes may indicate an important mechanism through which antiviral immunity is controlled.

Mitochondria are the cytoplasmic organelles where MAVS docks (Kawai et al., 2005; Meylan et al., 2005; Seth et al., 2005; Xu et al., 2005). On the one hand, MAVS in mitochondria receives signals from viral RNA-primed RIG-I; on the other hand, it activates antiviral kinase cascades to initiate IFN-I transcription through the TRAF3 adaptor (Kawai et al., 2005; Meylan et al., 2005; Seth et al., 2005; Xu et al., 2005). Hence, mitochondria serve as central platforms to transmit the IFN induction signal by tethering related signaling molecules together. Interestingly, our data showed that VSV infection induced CRM1-dependent TRIM24 translocation from the nucleus to mitochondria, where TRIM24 is associated with TRAF3 for downstream signaling activation. Because TRIM24 is constitutively bound with CRM1, viral infection did not affect its association with CRM1 but induced the translocation of TRIM24 to the cytoplasm through CRM1, a finding that needs further investigation to elucidate the mechanism controlling this action.

TRAF3 is a MAVS adaptor protein that undergoes K63-linked ubiquitination in mitochondria upon RNA virus infection, and this posttranslational modification of TRAF3 is essential in the virus-triggered induction of IFN-I (Häcker et al., 2011; Mao et al., 2010; Oganesyan et al., 2006). In contrast, the deubiquitination of TRAF3 induced by DUBA, OTUB1/2, or UCHL1 negatively regulates virus-induced IFN-I production (Karim et al., 2013; Kayagaki et al., 2007; Li et al., 2010). In contrast to the cellular apoptosis inhibitor cIAP1/2, which mediates both K48- and K63-linked ubiquitination of TRAF3 under specific circumstances, TRIM24 was found to be a direct E3 ligase that specifically induces the K63-linked ubiquitination of TRAF3 upon virus infection, and this action is independent of TRAF3 autoubiquitination activity. In addition, we also found that TRIM24-induced TRAF3 ubiquitination occurs at K429 and K436, and the knock-in data also confirmed the functional importance of ubiquitination at these two lysine residues in mediating virus-induced activation of IFN-I signaling. Interestingly, a published study showed that TRAF3 Y440 and Q442 are critical for its association with the TIM pocket of MAVS, and the Y440A/Q442A TRAF3 mutant blocked this interaction and thus impaired RNA virus–induced IFN-I production (Saha et al., 2006). Considering that K429 and K436 are physically close to Y440 and Q442 in the TRAF domain of TRAF3, it is highly likely that the K63-linked ubiquitination at these two lysine residues also facilitates the interaction of TRAF3 with MAVS, an association that was confirmed by our knock-in data showing that the K429/436R TRAF3 mutant failed to interact with MAVS and thus suppressed downstream antiviral signaling.

In summary, we found that RNA virus infection induced CRM1-dependent TRIM24 translocation from the nucleus to the mitochondria, where TRIM24 mediated the K63-linked ubiquitination of TRAF3 and thus activated the downstream antiviral transcription factor IRF3, which was translocated into the nucleus to initiate IFN-I gene transcription. In the meantime, activated IRF3 also bound to the promoter of *TRIM24* and directly inhibited its gene transcription, forming a negative feedback loop to restrain overactivation of antiviral signaling (Fig. 9). Therefore, targeting

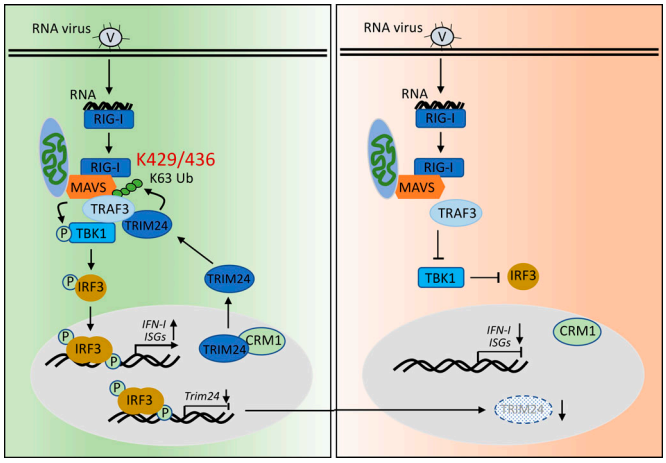

Figure 9. **The working model of TRIM24 in mediating antiviral immunity.** Upon RNA virus infection, TRIM24 induced a CRM1-dependent translocation from the nucleus to the mitochondria, where TRIM24 associated with TRAF3 and mediated its K63-linked ubiquitination at K429 and K436. This modification facilitated the association of TRAF3 with MAVS and TBK1, which promoted the phosphorylation and nuclear translocation of IRF3, resulting in promoted transcriptional activation of IFN-I genes. In the meantime, activated IRF3 directly bound to the promoter of TRIM24 to suppress its gene expression, forming a negative feedback loop to restrain overactivation of antiviral signaling.

TRIM24 may have a beneficial effect by boosting the host antiviral immune response and thus antagonizing RNA virus infection.

Materials and methods

Mice

TRIM24 floxed mice (previously described in Yu et al., 2019) were backcrossed with C57BL/6 mice for ≥6 generations. C57BL/6 background TRIM24 floxed mice were crossed with B6.C-Tg (CMV-Cre) 1Cgn/J mice (J006054; purchased from GemPharmatech Co.) to produce *TRIM24* total knockout mice (termed *TRIM24*-KO). In all experiments, WT littermate controls were used. All mice were maintained in a specific pathogen–free facility, and all animal experiments were in accordance with protocols approved by the institutional Biomedical Research Ethics Committee, Shanghai Institute of Nutrition and Health, Chinese Academy of Sciences, Shanghai, China.

Cells and viruses

TRAF3-KO MEFs were kindly provided by Dr. Shao-Cong Sun (MD Anderson Cancer Center, Houston, TX). *IRF3*-KO HEK293T were kindly provided by F. Hou (Shanghai Institute of Biochemistry and Cell Biology, Chinese Academy of Sciences). The cells were cultured at 37°C under 5% CO_2 in DMEM supplemented with 10% FBS, 100 U/ml penicillin, and 100 µg/ml streptomycin. SeV, VSV, VSV-GFP, and HSV-1 were also kindly provided by F. Hou (Zhu et al., 2019a).

Viral infection in vitro and in vivo

Cells were infected with VSV, HSV-1, or SeV at multiplicity of infection of 1 for the indicated times. For in vivo viral infection

studies, age- and sex-matched WT and *TRIM24*-KO mice were infected with VSV (1×10^8 PFU/mouse) via tail vein injection and monitored for survival status. Lungs from control or virus-infected mice were dissected, fixed in 4% paraformaldehyde, embedded in paraffin, sectioned, stained with H&E solution, and examined by light microscopy for histological changes. Serum cytokine production was measured by ELISA. mRNA expression of *Ifna4*, *Ifnb1*, and *VSV* in the lung and spleen was detected via real-time QPCR. VSVG protein expression in the lung and spleen was determined by immunoblot assay.

Plasmids, antibodies, and reagents

The cDNA encoding TRIM24 and its truncations were cloned from THP-1 cells and constructed into pcDNA vector. The expression vector encoding Flag-TRAF3, Flag-MAVS, Flag-TBK1, Flag-TRAF6, HA-tagged different types of ubiquitin, IFNβ luciferase reporter, and pRL-TK plasmids were kindly provided by Dr. Shao-Cong Sun. The expression vector encoding mutant Flag-TRAF3 C68A/H70A was kindly provided by Dr. Xiang He (Beijing Institute of Biotechnology, Beijing, China). For the generation of TRAF3 K369R, K429R, K436R, and K429/436R mutants, point mutations were constructed by site-directed mutagenesis. The expression vectors encoding Flag-RIGI-N and Flag-IRF3-5D were kindly provided by Dr. Chengjiang Gao (Shandong University School of Basic Medical Sciences, Shandong, China). The expression vector encoding CRM1 was kindly provided by Dr. Wenjun Liu (Institute of Microbiology, Chinese Academy of Sciences). All homemade and requested constructs were confirmed by DNA sequencing.

Antibodies for TRIM24 (14208-1-AP), GAPDH (60004-1-1G), TRAF3 (18099-1-AP) and MAVS (14341-1-AP) were from Proteintech. Antibodies for TRIM24 (C-4, sc-271266), Hsp60 (H-1, sc-13115), Lamin B (C-20, sc-6216), p65 (C-20, sc-372), IκBα (C-21, sc-371), p38 (H-147, sc-7149), Erk1 (K-23, sc-94), P-Erk (E-4, sc-7383), TRAF2 (C-20, SC-876), TRAF3 (H-122, sc-1828), CRM1 (H-7, sc-74455), IRF3 (FL-425, sc-9082), STAT1 (M-22, sc-592), ubiquitin (Ub; P4D1, sc-8017), c-Myc (9E10, sc-40), c-Myc-HRP (9E10, sc-40-HRP), and donkey anti-goat IgG (HRP, sc-2020) were from Santa Cruz. Antibodies for tubulin (2125S), VDAC (4661S), IRF3 (4302), Jnk (9252), TBK1 (3013), K63-linkage specific polyubiquitin (5621), MAVS (4983), p-IRF3 (29047), normal rabbit IgG (2729), p-Jnk (4668), p-p65 (3033), p-IκBα (2859), p-p38 (9215), and p-TBK1 (5483) were from Cell Signaling. Antibodies for β-actin (A2228), Flag (A8592), and VSVG (SAB4200695) were from Sigma-Aldrich. Antibody for GFP was from Abcam. Antibody for HA (2013819) was from Roche. Antibodies for Alexa Fluor Plus 488 conjugated mouse IgG (A32723) was from Thermo Fisher Scientific.

LPS (L3129) was purchased from Sigma-Aldrich; polyI:C was from InvivoGen; protein A/G magnetic beads (HY-K0202), Selinexor (KPT-330, HY-17536), and pyrrolidinedithiocarbamate ammonium (PDTC, HY-18738) were from MedChemExpress; PD98059 (S1177), SB203580 (S1076), and SP600125 (S1460) were from SelleckChem; and FastStart universal SYBR Green master mix (4913914001) was from Roche. LipoFiterTM Liposomal Transfection Reagent (HB-LF10001) was from Hanbio. HE staining kit (E607318-0200), Anti-Fade Mounting Medium (E675011), BSA (A602440), puromycin (A610593), proteinase K (A300491), and DAPI dihydrochloride (A606584) were from Sangon Biotech. FBS (10270), 2-mercaptoethanol (21985023), penicillin-streptomycin (15140-122), and GlutaMAX Supplement (35050-061) were from Gibco. DMEM/High Glucose (SH30243.01) and RPMI Medium Modified (SH30809.01) were from Hyclone. Protease inhibitor cocktail (B14001) and phosphatase inhibitor cocktail (B15001) were from Bimake. pMD18-T Vector (6011) and PrimeScript RT reagent kit (RR037A) were from Takara. TRIzol reagent (15596018), RNase A (8003089), Lipofectamine RNAiMAX (13778075), and Lipofectamine 3000 (L3000015) were from Thermo Fisher Scientific. BBL Thioglycollate Medium Brewer Modified (211716) was from BD. EZ-ChIP kit (17-371) and immobilon Western chemiluminescent HRP substrate (WBKLS0500) were from Millipore. Dual-luciferase reporter assay system (E1960) and TNT quick coupled transcription/translation systems (L1170) for in vitro protein expression were from Promega. Recombinant human UbcH5a/UBE2D1-ubiquitin charged (E2-800), recombinant human UbcH5a (uncharged, E2-616), recombinant human ubiquitin-activating Enzyme/UBE1 (E-305), recombinant human ubiquitin N-Terminal Biotin (UB-560), and Mg^{2+}-ATP (B-20) for in vitro ubiquitination assay were from Boston Biochem. ClonExpress II one step cloning kit (C112) and AxyPrep PCR cleanup kit (AP-PCR-250) were from Vazyme and Axygen, respectively. Recombinant human macrophage colony-stimulating factor (C417) and human IL-10 (CD04) were from Novoprotein. Recombinant mouse IFN Alpha 4 (12115) and mouse IFNβ ELISA Kit (42400) were from PBL. The mouse Macrophage Nucleofector Kit (VPA-1009) was purchased from Lonza.

Mouse and human macrophage preparation

Mouse BMDMs were prepared as previously described (Zhang et al., 2018). In brief, bone marrow cells isolated from mouse tibia and femur were cultured in 10-cm dishes with DMEM containing 20% FBS and L929 conditional medium. After 4–5 d of culture, the adherent macrophages were detached and seeded into culture plates for further experiments. For the preparation of peritoneal macrophages, 4% thioglycolate (BD) was i.p. injected into 6–8-wk-old WT and *TRIM24* KO mice. After 4–5 d, mice were sacrificed, and the peritoneal cavity was lavaged with DMEM medium. The peritoneal cells were collected by centrifugation and seeded in the dish. Macrophages were allowed to adhere for 4 h, washed with fresh medium to remove unattached cells, and incubated overnight.

Human PBMC-derived macrophages were prepared as previously described (Jin and Kruth, 2016). Briefly, PBMCs isolated from human peripheral blood of healthy donors were cultured in RPMI 1640 with 2 mM L-glutamine, 50 ng/ml M-CSF, 25 ng/ml IL-10, and 10% FBS. After monocytes differentiated and proliferated sufficiently to become confluent, which required ∼6 d of culture, macrophages were detached for further experiments. All human blood samples were collected after informed consent was obtained, and the related experiments were in accordance with protocols approved by the Institutional Biomedical Research Ethics Committee, Shanghai Institute of Nutrition and Health, Chinese Academy of Sciences.

Virus titer assay

Viral titer was determined by using a plaque assay as previously described (Zhu et al., 2019a). In brief, HEK293T cells in 6-well plates were infected with serial dilutions of the recovered VSV for 1 h. The infected cells were overlaid with 1% soft agar dissolved in DMEM and incubated for 48 h. Plates were stained with 0.1% crystal violet in DMEM to display plaques, which were then quantitated.

Native PAGE

Macrophages and HEK293T cells that were left uninfected or infected with VSV were washed and then harvested with 50 µl ice-cold lysis buffer (50 mM Tris-HCl, pH 8.0, 150 mM NaCl, and 1% NP-40 containing protease inhibitors). After centrifugation at 13,000 *g* for 5 min, supernatant protein was quantified and diluted with 2× native PAGE sample buffer (125 mM Tris-HCl, pH 6.8, 30% glycerol, and 0.01% bromophenol blue), and then applied to a prerun 6% native gel for separation. After electrophoresis, proteins were transferred onto a nitrocellulose membrane for immunoblotting.

Real-time QPCR

The expression of mRNA was examined by using real-time QPCR as previously described (Fan et al., 2019). In brief, total RNA was extracted by TRIzol reagent according to the manufacturer's protocol. cDNA was synthesized using the PrimeScript RT Reagent Kit (Takara). QPCR was performed by using SYBR Green Master mix (Roche). The relative expression of genes was calculated by a standard curve method and normalized to the expression level of *Actb*. Gene-specific PCR primers are listed in Table S1.

Gene knockdown in macrophages and HEK293T cells

For knockdown of *TRIM24* genes in mouse iBMDMs, the pLKO.1 vectors containing shRNA sequences targeting specific genes along with lentiviral packaging vectors, psPAX2 and pMD2, were transfected into HEK293T cells with Lipofectamine 3000. After 48 h, the lentiviral supernatants were collected for the infection of mouse iBMDM. The infected cells were selected with puromycin (8 µg/ml) for 48 h and examined for knockdown efficiency by immunoblotting. For knockdown of *TRIM24* in human PBMC-derived macrophages and HEK293T cells, siRNA targeting *TRIM24* (siTRIM24) or negative control (siControl) were transfected into cells with Lipofectamine RNAiMAX. For knockdown of E3 ligase or DUB genes in iBMDM, siRNA targeting the indicated genes or negative control were transfected into cells.

Immunofluorescence staining

Cells were fixed for 10 min with 4% cold paraformaldehyde and then permeabilized for 5 min with 0.2% Triton X-100. After blocking with 2% BSA in PBS containing 0.5% Tween-20, cells were stained with specific primary antibodies, followed by blotting with fluorescent conjugated secondary antibody. Nuclei were labeled with DAPI (Sangon Biotech). The stained cells were visualized and photographed with ZEISS Cell Observer.

RNA-sequencing analysis

Total RNA was extracted from VSV-infected or uninfected BMDMs and subjected to RNA-sequencing analysis by BGI Tech Solutions. The raw transcriptomic reads were mapped to a reference genome (GRCm38/mm10) with Bowtie. Gene expression levels were quantified with the RSEM software package. Significantly affected E3 ligase or DUB genes were acquired by setting a threshold with corrected $P < 0.005$ and $\log2 \leq -1.5$ or $\log2 \geq 1.5$, and are presented as heat maps.

Luciferase reporter assay

IFNβ luciferase reporter was cotransfected with pRL-TK, and other expression vectors where indicated, into HEK293T cells by using LipoFiterTM Transfection Reagent (HanBio). IFNβ transcriptional activity was measured with Dual-Luciferase Reporter Assay System (Promega), and the relative light units of chemiluminescence were measured with LB 9508 Lumat3 (Berthold Technologies).

Coimmunoprecipitation and immunoblot analysis

For coimmunoprecipitation assays, cells were lysed with radioimmunoprecipitation assay (RIPA) buffer containing protease/phosphatase inhibitors. The whole-cell lysates were incubated with desired antibodies, and the target protein was then pulled down with protein A/G magnetic beads. For immunoblot analysis, immunoprecipitates or whole-cell lysates were resolved using SDS-PAGE, transferred to nitrocellulose membranes (Millipore), and then blotted with specific primary and secondary antibodies. Immunoblots were visualized using the Immobilon Western chemiluminescent HRP substrate (Millipore) with luminescent imaging workstation (Tanon). In some experiments, the mitochondria proteins were isolated by using Qproteome Mitochondria Isolation Kit (Qiagen) according to the manufacturer's instructions, and then applied for immunoblot assay.

Ubiquitination assay

The in vivo ubiquitination assay was performed as previously described (Liu et al., 2018; Zhang et al., 2019). In brief, VSV infected or uninfected macrophages or HEK293T cells transfected with the desired plasmids were lysed with cell lysis RIPA buffer (50 mM Tris-HCl, pH 7.4, 150 mM NaCl, 1% NP-40, 0.5% sodium deoxycholate, and 1 mM EDTA) containing protease inhibitor and *N*-ethylmaleimide (Sigma-Aldrich). After saving some cell extracts for input analysis, the remaining cell extracts were added to SDS to a final concentration of 1% and then boiled at 100°C for 5 min, which dissociated all the potential protein complexes under such denaturing conditions. The boiled cell extracts were diluted with RIPA buffer until the SDS concentration was 0.1%, precleaned with protein A/B–coupled agarose beads, and then incubated with specific immunoprecipitation antibody on a shaker under denaturing conditions (0.1% SDS) at 4°C overnight. The next day, the immunoprecipitated proteins were collected by incubation with protein A/B–coupled agarose beads on a shaker at 4°C for 2 h, washed with RIPA buffer containing protease inhibitors, PMSF, and *N*-ethylmaleimide, boiled at 100°C for 5 min, and then loaded to run SDS-PAGE. The

immunoprecipitates were immunoblotted with anti-ubiquitin or indicated antibodies.

For in vitro ubiquitination assay, TRAF3 and TRIM24 proteins were expressed in vitro with the TNT Quick Coupled Transcription/Translation Systems (Promega). In vitro ubiquitination assays were performed with the Ubiquitination Kit (Boston Biochem) according to the manufacturer's instructions.

Mass spectrum

Flag-TRAF3, HA-Ub, and Myc-TRIM24 expression plasmids were cotransfected into HEK293T cells. Cells were harvested 48 h after transfection, and the lysates were immunoprecipitated with anti-Flag antibody. After washing, the eluted samples were resolved with SDS-PAGE, followed by Coomassie brilliant blue staining. The sample of TRAF3 band was cut and sent to process with mass spectrum analysis using a QE1 system at the National Facility for Protein Science in Shanghai, Zhangjiang Lab.

ChIP-QPCR assay

The ChIP assay procedure was modified from the manufacturer's instructions (EZ-ChIP, Millipore). Briefly, isolated peritoneal macrophages (~1 × 10^7 cells) were fixed with 1% formaldehyde (Sigma-Aldrich) at room temperature for 10 min in 10 ml medium, followed by quenching with 125 mM glycine. Nuclear extracts were sonicated with Covaris E220 for 660 s. After preclearing with normal IgG for 1 h, the sonicated cell lysates were immunoprecipitated with the IRF3 antibody overnight on a nutator at 4°C. The next day, protein A/G magnetic beads were added, and cell lysates were incubated on a nutator for another 2 h. After washing with buffers, chromatin was eluted from the protein/DNA complex and digested with proteinase K and RNaseA at 65°C overnight to reverse cross-links. The freed DNA was purified with AxyPrep PCR cleanup kit (Axygen) and subjected to QPCR analysis with SYGR Green master mix. All sequences of primers for ChIP-QPCR are shown in Table S1.

CRISPR-Cas9–mediated genome editing

To create TRAF3-K429/436R gene-targeted alleles in HEK293T cells, the small guide RNA (sgRNA) sequences near the codon encoding Lys429/436 were chosen on the basis of their specificity scores (https://crispr.mit.edu/). The sgRNA sequences were then cloned into the lentiCRISPRv2 plasmid (Addgene). The repair template harboring ~1-kb homology arms flanking the TRAF3 K429/436 codon was amplified from the genomic DNA of 293T cells and cloned into pMD18-T Vector (Takara). The mutation encoding K429/436R (AAG→AGG) was then introduced into the repair template. To avoid the cleavage of the repair template by Cas9, an additional synonymous mutation was designed to make the repair template sequence different from the sgRNA sequences. The lentiCRISPRv2 plasmids and repair template were cotransfected into HEK293T cells. 48 h later, the cells were treated with 5 µg/ml puromycin for 3 d to remove the cells without transfection, and single cells were seeded into separate wells of 96-well plates. After clonal expansion, genomic DNA was amplified by PCR using primers flanking the TRAF3 K429/436 codon. The PCR products were then sequenced to validate the TRAF3 K429/436R mutation in both alleles. The sgRNA sequence is human TRAF3 K429/436R sgRNA: 5′-GGAAGCAGGAGGCCGTCATG-3′.

Statistical analysis

The data are shown as mean ± SEM, and unless otherwise indicated, all the presented data are representative results of at least three independent repeats. Statistical analysis was performed with Prism 6 (GraphPad), and the statistics were analyzed by two-tailed Student's *t* test or one-way or two-way ANOVA as indicated. Differences considered to be significant at $P < 0.05$ are indicated by *, those at $P < 0.01$ are indicated by **.

Data availability

The RNA-sequencing data have been deposited into the Gene Expression Omnibus (accession code GSE136363). All other data supporting the findings of this study are available from the corresponding author on reasonable request.

Online supplemental material

Fig. S1 shows the identification of TRIM24 deletion efficiency in different cells of *TRIM24*-KO mice, and that TRIM24 positively regulates VSV-induced ISG genes and is dispensable for the induction of proinflammatory genes Fig. S2 shows that TRIM24 facilitates the association of TRAF3 with MAVS and TBK1. Fig. S3 shows potential ubiquitination sites of TRAF3 identified by mass spectrum. Fig. S4 shows that TRAF3 K429/K436 are critical for the VSV-induced IFN-I.

Acknowledgments

We thank Dr. Shao-Cong Sun (MD Anderson Cancer Center, Houston, TX), Dr. Xiang He (Beijing Institute of Biotechnology, Beijing, China), and Dr. Chengjiang Gao (Shandong University School of Basic Medical Sciences, Shandong, China) for the generous gift of plasmids.

This research was supported by the grants from the National Key R&D Program of China (2018YFA0107201, 2018YFA0902703), the Strategic Priority Research Program of the Chinese Academy of Sciences (XDB39000000 and XDB19000000), the Key Research Program of the Chinese Academy of Sciences (KFZD-SW-216), the National Natural Science Foundation of China (81770567 and 81825018), the Thousand Young Talents Plan of China, and Chinese Academy of Sciences Key Laboratory of Tissue Microenvironment and Tumor.

Author contributions: Q. Zhu designed and performed the experiments, prepared the figures, and wrote part of the manuscript; T. Yu, S. Gan, Y. Wang, Y. Pei, Q. Zhao, S. Pei, S. Hao, J. Yuan, and J. Xu contributed to the experiments; C. Peng and P. Wu contributed to mass spectrum analysis; F. Hou provided the DNA and RNA virus and *IRF3*-KO HEK293T cells and contributed to virus titer experiments; X. Wu provided *TRAF3*-KO MEFs; J. Qin contributed to plasmids and critical editing; Y. Xiao designed and supervised this study, prepared the figures, and wrote the manuscript.

Disclosures: The authors declare no competing interests exist.

Submitted: 4 November 2019
Revised: 26 January 2020
Accepted: 3 March 2020

References

Arimoto, K., H. Takahashi, T. Hishiki, H. Konishi, T. Fujita, and K. Shimotohno. 2007. Negative regulation of the RIG-I signaling by the ubiquitin ligase RNF125. *Proc. Natl. Acad. Sci. USA.* 104:7500–7505. https://doi.org/10.1073/pnas.0611551104

Castanier, C., N. Zemirli, A. Portier, D. Garcin, N. Bidère, A. Vazquez, and D. Arnoult. 2012. MAVS ubiquitination by the E3 ligase TRIM25 and degradation by the proteasome is involved in type I interferon production after activation of the antiviral RIG-I-like receptors. *BMC Biol.* 10:44. https://doi.org/10.1186/1741-7007-10-44

Chan, Y.K., and M.U. Gack. 2016. A phosphomimetic-based mechanism of dengue virus to antagonize innate immunity. *Nat. Immunol.* 17:523–530. https://doi.org/10.1038/ni.3393

Chiang, J.J., K.M.J. Sparrer, M. van Gent, C. Lässig, T. Huang, N. Osterrieder, K.P. Hopfner, and M.U. Gack. 2018. Viral unmasking of cellular 5S rRNA pseudogene transcripts induces RIG-I-mediated immunity. *Nat. Immunol.* 19:53–62. https://doi.org/10.1038/s41590-017-0005-y

Cui, J., Y. Song, Y. Li, Q. Zhu, P. Tan, Y. Qin, H.Y. Wang, and R.F. Wang. 2014. USP3 inhibits type I interferon signaling by deubiquitinating RIG-I-like receptors. *Cell Res.* 24:400–416. https://doi.org/10.1038/cr.2013.170

Dalrymple, N.A., V. Cimica, and E.R. Mackow. 2015. Dengue Virus NS Proteins Inhibit RIG-I/MAVS Signaling by Blocking TBK1/IRF3 Phosphorylation: Dengue Virus Serotype 1 NS4A Is a Unique Interferon-Regulating Virulence Determinant. *MBio.* 6:e00553-15. https://doi.org/10.1128/mBio.00553-15

Fan, K.Q., Y.Y. Li, H.L. Wang, X.T. Mao, J.X. Guo, F. Wang, L.J. Huang, Y.N. Li, X.Y. Ma, Z.J. Gao, et al. 2019. Stress-Induced Metabolic Disorder in Peripheral CD4$^+$ T Cells Leads to Anxiety-like Behavior. *Cell.* 179:864–879.e19. https://doi.org/10.1016/j.cell.2019.10.001

Friedman, C.S., M.A. O'Donnell, D. Legarda-Addison, A. Ng, W.B. Cárdenas, J.S. Yount, T.M. Moran, C.F. Basler, A. Komuro, C.M. Horvath, et al. 2008. The tumour suppressor CYLD is a negative regulator of RIG-I-mediated antiviral response. *EMBO Rep.* 9:930–936. https://doi.org/10.1038/embor.2008.136

Gack, M.U., Y.C. Shin, C.H. Joo, T. Urano, C. Liang, L. Sun, O. Takeuchi, S. Akira, Z. Chen, S. Inoue, and J.U. Jung. 2007. TRIM25 RING-finger E3 ubiquitin ligase is essential for RIG-I-mediated antiviral activity. *Nature.* 446:916–920. https://doi.org/10.1038/nature05732

Goubau, D., S. Deddouche, and C. Reis e Sousa. 2013. Cytosolic sensing of viruses. *Immunity.* 38:855–869. https://doi.org/10.1016/j.immuni.2013.05.007

Häcker, H., P.H. Tseng, and M. Karin. 2011. Expanding TRAF function: TRAF3 as a tri-faced immune regulator. *Nat. Rev. Immunol.* 11:457–468. https://doi.org/10.1038/nri2998

He, Z., X. Zhu, W. Wen, J. Yuan, Y. Hu, J. Chen, S. An, X. Dong, C. Lin, J. Yu, et al. 2016. Dengue Virus Subverts Host Innate Immunity by Targeting Adaptor Protein MAVS. *J. Virol.* 90:7219–7230. https://doi.org/10.1128/JVI.00221-16

Heaton, S.M., N.A. Borg, and V.M. Dixit. 2016. Ubiquitin in the activation and attenuation of innate antiviral immunity. *J. Exp. Med.* 213:1–13. https://doi.org/10.1084/jem.20151531

Hutten, S., and R.H. Kehlenbach. 2007. CRM1-mediated nuclear export: to the pore and beyond. *Trends Cell Biol.* 17:193–201. https://doi.org/10.1016/j.tcb.2007.02.003

Jin, X., and H.S. Kruth. 2016. Culture of Macrophage Colony-stimulating Factor Differentiated Human Monocyte-derived Macrophages. *J. Vis. Exp.* (112):54244.

Karim, R., B. Tummers, C. Meyers, J.L. Biryukov, S. Alam, C. Backendorf, V. Jha, R. Offringa, G.J. van Ommen, C.J. Melief, et al. 2013. Human papillomavirus (HPV) upregulates the cellular deubiquitinase UCHL1 to suppress the keratinocyte's innate immune response. *PLoS Pathog.* 9:e1003384. https://doi.org/10.1371/journal.ppat.1003384

Kawai, T., K. Takahashi, S. Sato, C. Coban, H. Kumar, H. Kato, K.J. Ishii, O. Takeuchi, and S. Akira. 2005. IPS-1, an adaptor triggering RIG-I- and Mda5-mediated type I interferon induction. *Nat. Immunol.* 6:981–988. https://doi.org/10.1038/ni1243

Kayagaki, N., Q. Phung, S. Chan, R. Chaudhari, C. Quan, K.M. O'Rourke, M. Eby, E. Pietras, G. Cheng, J.F. Bazan, et al. 2007. DUBA: a deubiquitinase that regulates type I interferon production. *Science.* 318:1628–1632. https://doi.org/10.1126/science.1145918

Khan, R., A. Khan, A. Ali, and M. Idrees. 2019. The interplay between viruses and TRIM family proteins. *Rev. Med. Virol.* 29:e2028. https://doi.org/10.1002/rmv.2028

Li, S., H. Zheng, A.P. Mao, B. Zhong, Y. Li, Y. Liu, Y. Gao, Y. Ran, P. Tien, and H.B. Shu. 2010. Regulation of virus-triggered signaling by OTUB1- and OTUB2-mediated deubiquitination of TRAF3 and TRAF6. *J. Biol. Chem.* 285:4291–4297. https://doi.org/10.1074/jbc.M109.074971

Liu, J., X. Huang, S. Hao, Y. Wang, M. Liu, J. Xu, X. Zhang, T. Yu, S. Gan, D. Dai, et al. 2018. Peli1 negatively regulates noncanonical NF-κB signaling to restrain systemic lupus erythematosus. *Nat. Commun.* 9:1136. https://doi.org/10.1038/s41467-018-03530-3

Manokaran, G., E. Finol, C. Wang, J. Gunaratne, J. Bahl, E.Z. Ong, H.C. Tan, O.M. Sessions, A.M. Ward, D.J. Gubler, et al. 2015. Dengue subgenomic RNA binds TRIM25 to inhibit interferon expression for epidemiological fitness. *Science.* 350:217–221. https://doi.org/10.1126/science.aab3369

Mao, A.P., S. Li, B. Zhong, Y. Li, J. Yan, Q. Li, C. Teng, and H.B. Shu. 2010. Virus-triggered ubiquitination of TRAF3/6 by cIAP1/2 is essential for induction of interferon-beta (IFN-beta) and cellular antiviral response. *J. Biol. Chem.* 285:9470–9476. https://doi.org/10.1074/jbc.M109.071043

Meylan, E., J. Curran, K. Hofmann, D. Moradpour, M. Binder, R. Bartenschlager, and J. Tschopp. 2005. Cardif is an adaptor protein in the RIG-I antiviral pathway and is targeted by hepatitis C virus. *Nature.* 437:1167–1172. https://doi.org/10.1038/nature04193

Oganesyan, G., S.K. Saha, B. Guo, J.Q. He, A. Shahangian, B. Zarnegar, A. Perry, and G. Cheng. 2006. Critical role of TRAF3 in the Toll-like receptor-dependent and -independent antiviral response. *Nature.* 439:208–211. https://doi.org/10.1038/nature04374

Pauli, E.K., Y.K. Chan, M.E. Davis, S. Gableske, M.K. Wang, K.F. Feister, and M.U. Gack. 2014. The ubiquitin-specific protease USP15 promotes RIG-I-mediated antiviral signaling by deubiquitylating TRIM25. *Sci. Signal.* 7:ra3. https://doi.org/10.1126/scisignal.2004577

Saha, S.K., E.M. Pietras, J.Q. He, J.R. Kang, S.Y. Liu, G. Oganesyan, A. Shahangian, B. Zarnegar, T.L. Shiba, Y. Wang, and G. Cheng. 2006. Regulation of antiviral responses by a direct and specific interaction between TRAF3 and Cardif. *EMBO J.* 25:3257–3263. https://doi.org/10.1038/sj.emboj.7601220

Seth, R.B., L. Sun, C.K. Ea, and Z.J. Chen. 2005. Identification and characterization of MAVS, a mitochondrial antiviral signaling protein that activates NF-kappaB and IRF 3. *Cell.* 122:669–682. https://doi.org/10.1016/j.cell.2005.08.012

Tisserand, J., K. Khetchoumian, C. Thibault, D. Dembélé, P. Chambon, and R. Losson. 2011. Tripartite motif 24 (Trim24/Tif1α) tumor suppressor protein is a novel negative regulator of interferon (IFN)/signal transducers and activators of transcription (STAT) signaling pathway acting through retinoic acid receptor α (Rarα) inhibition. *J. Biol. Chem.* 286:33369–33379. https://doi.org/10.1074/jbc.M111.225680

Tseng, P.H., A. Matsuzawa, W. Zhang, T. Mino, D.A. Vignali, and M. Karin. 2010. Different modes of ubiquitination of the adaptor TRAF3 selectively activate the expression of type I interferons and proinflammatory cytokines. *Nat. Immunol.* 11:70–75. https://doi.org/10.1038/ni.1819

van Gent, M., K.M.J. Sparrer, and M.U. Gack. 2018. TRIM Proteins and Their Roles in Antiviral Host Defenses. *Annu. Rev. Virol.* 5:385–405. https://doi.org/10.1146/annurev-virology-092917-043323

Versteeg, G.A., R. Rajsbaum, M.T. Sánchez-Aparicio, A.M. Maestre, J. Valdiviezo, M. Shi, K.-S. Inn, A. Fernandez-Sesma, J. Jung, and A. García-Sastre. 2013. The E3-ligase TRIM family of proteins regulates signaling pathways triggered by innate immune pattern-recognition receptors. *Immunity.* 38:384–398. https://doi.org/10.1016/j.immuni.2012.11.013

Wang, G., Y. Gao, L. Li, G. Jin, Z. Cai, J.I. Chao, and H.K. Lin. 2012. K63-linked ubiquitination in kinase activation and cancer. *Front. Oncol.* 2:5. https://doi.org/10.3389/fonc.2012.00005

Xu, L.G., Y.Y. Wang, K.J. Han, L.Y. Li, Z. Zhai, and H.B. Shu. 2005. VISA is an adapter protein required for virus-triggered IFN-beta signaling. *Mol. Cell.* 19:727–740. https://doi.org/10.1016/j.molcel.2005.08.014

Yan, J., Q. Li, A.P. Mao, M.M. Hu, and H.B. Shu. 2014. TRIM4 modulates type I interferon induction and cellular antiviral response by targeting RIG-I for K63-linked ubiquitination. *J. Mol. Cell Biol.* 6:154–163. https://doi.org/10.1093/jmcb/mju005

Ye, J.S., N. Kim, K.J. Lee, Y.R. Nam, U. Lee, and C.H. Joo. 2014. Lysine 63-linked TANK-binding kinase 1 ubiquitination by mindbomb E3 ubiquitin protein ligase 2 is mediated by the mitochondrial antiviral signaling protein. *J. Virol.* 88:12765–12776. https://doi.org/10.1128/JVI.02037-14

Yoshida, R., G. Takaesu, H. Yoshida, F. Okamoto, T. Yoshioka, Y. Choi, S. Akira, T. Kawai, A. Yoshimura, and T. Kobayashi. 2008. TRAF6 and MEKK1 play a pivotal role in the RIG-I-like helicase antiviral pathway. *J. Biol. Chem.* 283:36211–36220. https://doi.org/10.1074/jbc.M806576200

Yu, T., S. Gan, Q. Zhu, D. Dai, N. Li, H. Wang, X. Chen, D. Hou, Y. Wang, Q. Pan, et al. 2019. Modulation of M2 macrophage polarization by the crosstalk between Stat6 and Trim24. *Nat. Commun.* 10:4353. https://doi.org/10.1038/s41467-019-12384-2

Zhang, X., Y. Wang, J. Yuan, N. Li, S. Pei, J. Xu, X. Luo, C. Mao, J. Liu, T. Yu, et al. 2018. Macrophage/microglial Ezh2 facilitates autoimmune inflammation through inhibition of Socs3. *J. Exp. Med.* 215:1365–1382. https://doi.org/10.1084/jem.20171417

Zhang, Y., R.B. Liu, Q. Cao, K.Q. Fan, L.J. Huang, J.S. Yu, Z.J. Gao, T. Huang, J.Y. Zhong, X.T. Mao, et al. 2019. USP16-mediated deubiquitination of calcineurin A controls peripheral T cell maintenance. *J. Clin. Invest.* 129: 2856–2871. https://doi.org/10.1172/JCI123801

Zhong, B., L. Zhang, C. Lei, Y. Li, A.P. Mao, Y. Yang, Y.Y. Wang, X.L. Zhang, and H.B. Shu. 2009. The ubiquitin ligase RNF5 regulates antiviral responses by mediating degradation of the adaptor protein MITA. *Immunity.* 30:397–407. https://doi.org/10.1016/j.immuni.2009.01.008

Zhou, P., X. Ding, X. Wan, L. Liu, X. Yuan, W. Zhang, X. Hui, G. Meng, H. Xiao, B. Li, et al. 2018. MLL5 suppresses antiviral innate immune response by facilitating STUB1-mediated RIG-I degradation. *Nat. Commun.* 9:1243. https://doi.org/10.1038/s41467-018-03563-8

Zhu, W., J. Li, R. Zhang, Y. Cai, C. Wang, S. Qi, S. Chen, X. Liang, N. Qi, and F. Hou. 2019a. TRAF3IP3 mediates the recruitment of TRAF3 to MAVS for antiviral innate immunity. *EMBO J.* 38:e102075. https://doi.org/10.15252/embj.2019102075

Zhu, Z., P. Li, F. Yang, W. Cao, X. Zhang, W. Dang, X. Ma, H. Tian, K. Zhang, M. Zhang, et al. 2019b. Peste des Petits Ruminants Virus Nucleocapsid Protein Inhibits Beta Interferon Production by Interacting with IRF3 To Block Its Activation. *J. Virol.* 93:e00362-19. https://doi.org/10.1128/JVI.00362-19

Supplemental material

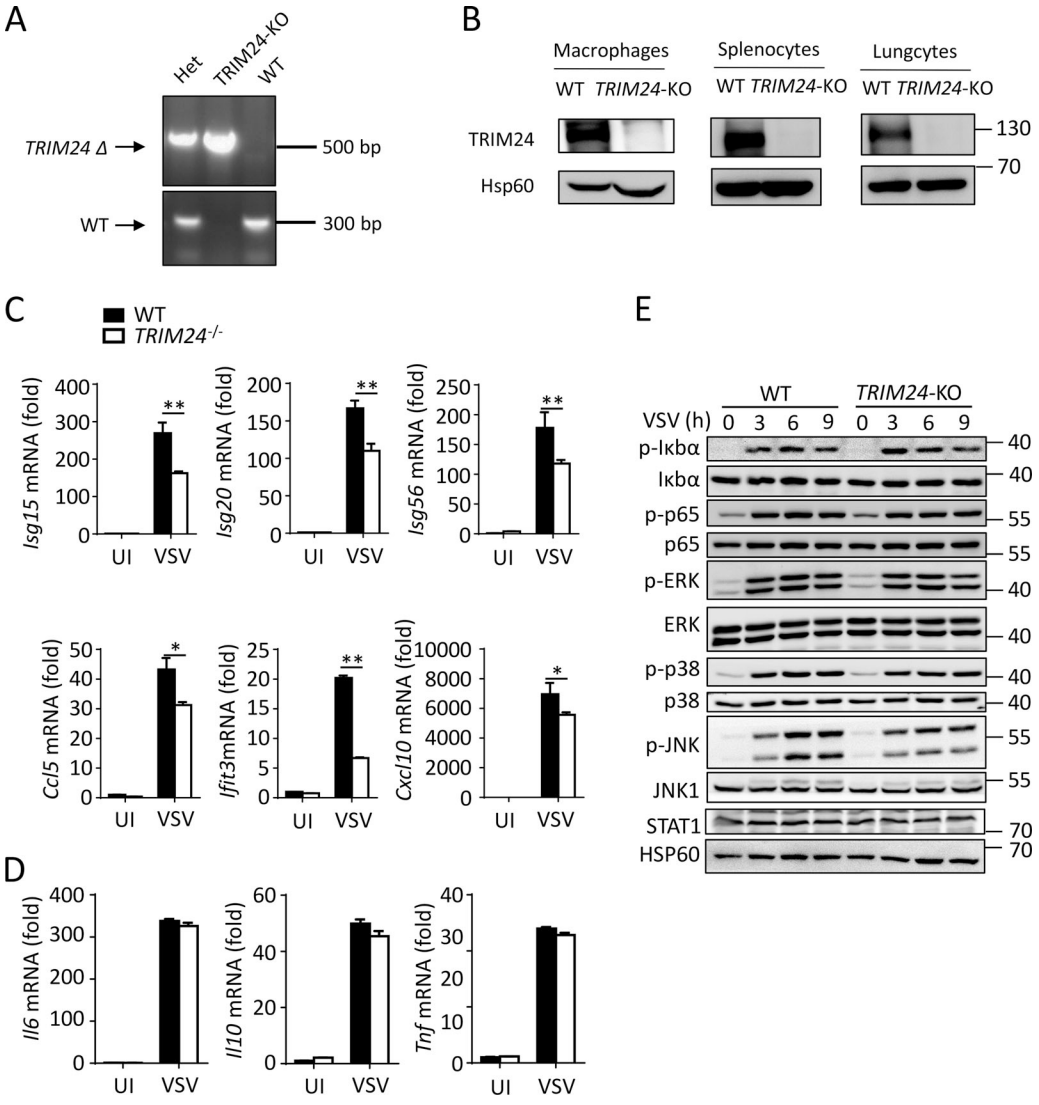

Figure S1. **TRIM24 positively regulates VSV-induced ISG genes and is dispensable for the induction of proinflammatory genes. (A)** Genotyping PCR analysis of WT, Het, and *TRIM24*-KO mice. **(B)** Immunoblot analysis of TRIM24 and Hsp60 (loading control) protein expression in macrophages, splenocytes, and lungcytes isolated from WT and *TRIM24*-KO mice. **(C and D)** QPCR analysis of *Isg15*, *Isg20*, *Isg56*, *Ccl5*, *Ifit3vCxxl10* (A), *Il6*, *Il10*, and *Tnf* mRNA (B) in WT and *TRIM24*-KO peritoneal macrophages left uninfected (UI) or infected with VSV for 12 h. **(E)** Immunoblot of p-Iκbα, p-p65, p-ERK, p-p38, p-JNK, and total Iκbα, p65, ERK, p38, and JNK in WT and *TRIM24*-KO peritoneal macrophages left uninfected or infected with VSV for the indicated times.

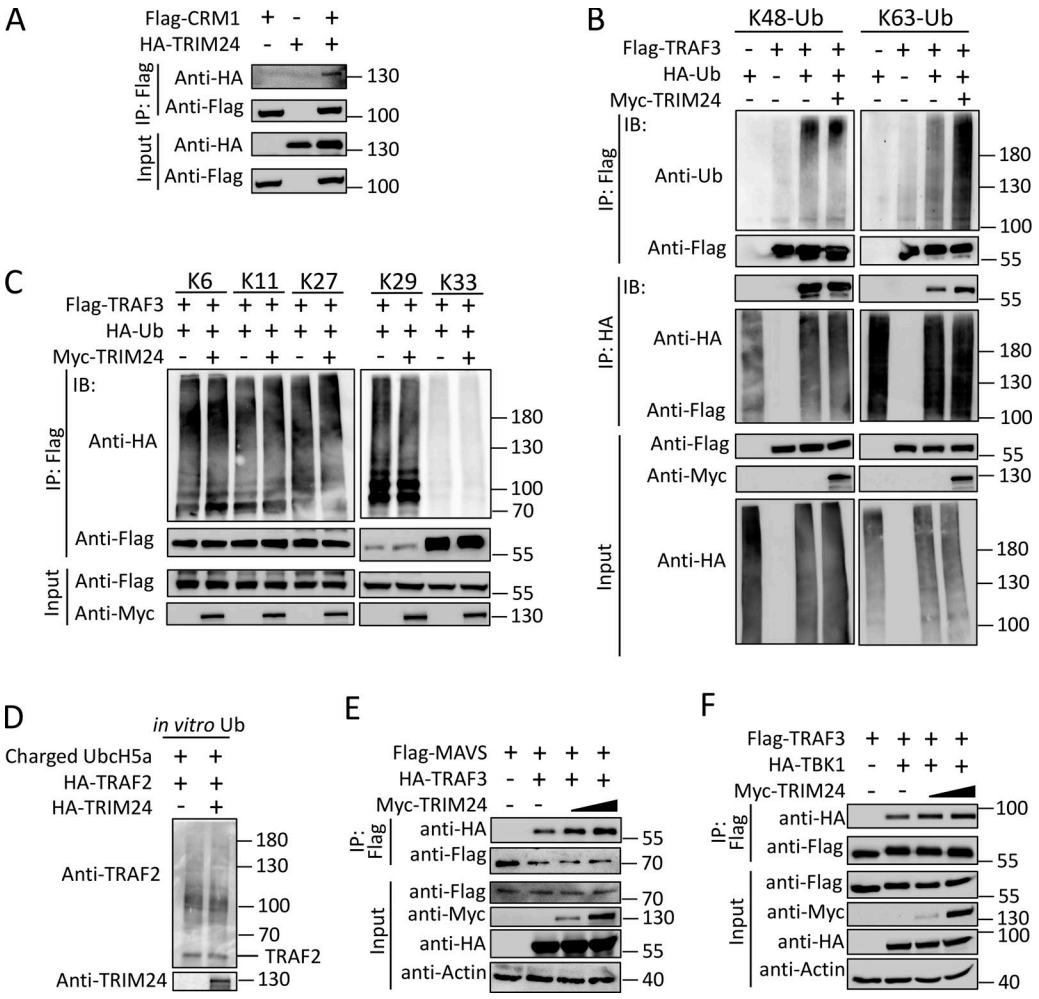

Figure S2. **TRIM24 facilitates the association of TRAF3 with MAVS and TBK1. (A)** Immunoblot analysis of TRIM24–CRM1 interaction in HEK293T cells transfected with the indicated expression vectors, assessed by immunoprecipitation (IP) with anti-Flag and anti-HA and immunoblot with anti-HA and anti-Flag without immunoprecipitation. **(B)** Ubiquitination of TRAF3 in HEK293T cells transfected with the indicated expression vectors, assessed by immunoblot analysis with anti-HA after immunoprecipitation with anti-Flag or by immunoblot analysis with input proteins in lysates without immunoprecipitation. **(C)** In vitro ubiquitination assay of TRAF2 ubiquitination after a mixture reaction of ubiquitin-charged E2 (UbcH5a) in vitro translated HA-TRAF2, and with or without HA-TRIM24 proteins, assessed by immunoblot analysis with anti-TRAF2 and anti-TRIM24. **(D and E)** Immunoblot analysis of TRAF3–MAVS (D) or TRAF3–TBK1 (E) interactions in HEK293T cells transfected with the indicated expression vectors encoding TRAF3, MAVS, TBK1, and different doses of TRIM24, assessed by IP with anti-Flag and immunoblot with anti-HA and anti-Flag, and by immunoblot analysis with input proteins in lysates without immunoprecipitation.

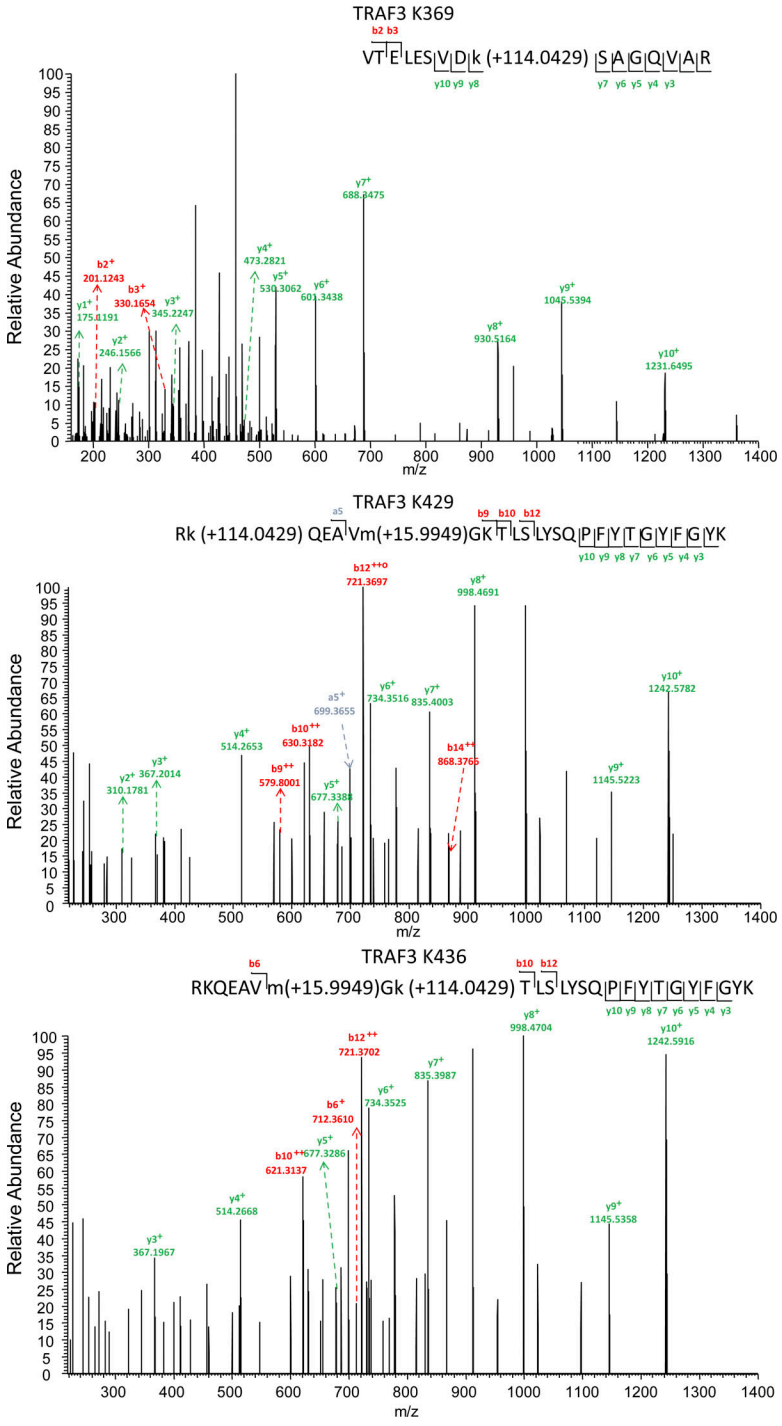

Figure S3. **Mass spectrum showing the potential ubiquitination sites of TRAF3 after immunoprecipitation of TRAF3 in HEK293T cells transfected with TRAF3, TRIM24, and ubiquitin.**

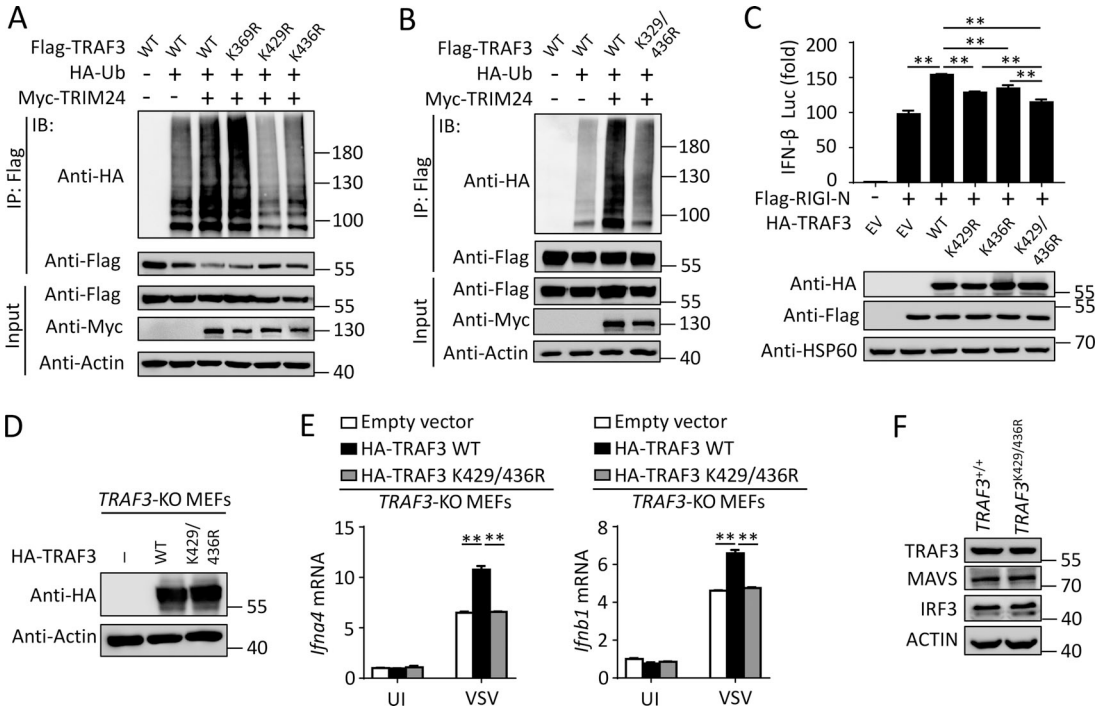

Figure S4. **TRAF3 K429/K436 are critical for the induction of IFN-I. (A and B)** Ubiquitination of TRAF3 in HEK293T cells transfected with the indicated expression vectors, assessed by immunoblot analysis with anti-HA after immunoprecipitation with anti-Flag or by immunoblot analysis with input proteins in lysates without immunoprecipitation. **(C)** IFNβ luciferase activity in HEK293T cells transfected with the indicated expression vectors (upper), and immunoblot analysis of Flag-RIGI-N, HA-TRAF3, and its site mutants and HSP60 (below). **(D)** Immunoblot analysis of HA-TRAF3 in *TRAF3*-KO MEFs reconstituted with empty vector (EV), HA-TRAF3-WT, or HA-TRAF3-K429/436R. **(E and F)** QPCR analysis of *Ifna4* and *Ifnb1* in *TRAF3*-KO MEFs reconstituted with EV, HA-TRAF3-WT, or HA-TRAF3-K429/436R, then left uninfected (UI) or infected with VSV for 6 h. **(F)** Immunoblot analysis of endogenous protein expression of TRAF3, MAVS, and IRF3 in *TRAF3*$^{+/+}$ and *TRAF3*$^{K429/436R}$ HEK293T cells.

Table S1 is provided online as a Word document and lists primers used for real-time QPCR.